Journal of Transportation Technologies, 2022, 12, 498-532
https://www.scirp.org/journal/jtts
ISSN Online: 2160-0481
ISSN Print: 2160-0473

Vehicle Dynamics with Additional Entry Lane of a Roundabout

Nikolay Nazaryan[1], Clara Fang[2*]

[1]College of Engineering, Technology and Architecture, University of Hartford, West Hartford, USA
[2]Department of Civil, Environmental and Biomedical Engineering, College of Engineering, Technology and Architecture, University of Hartford, West Hartford, USA
Email:*fang@hartford.edu

How to cite this paper: Nazaryan, N. and Fang, C. (2022) Vehicle Dynamics with Additional Entry Lane of a Roundabout. *Journal of Transportation Technologies*, **12**, 498-532.
https://doi.org/10.4236/jtts.2022.123030

Received: June 7, 2022
Accepted: July 25, 2022
Published: July 28, 2022

Abstract

This research is dedicated to the study of dynamics of vehicles moving through the additional entry lanes of a roundabout. Using the data created on the base of that model the constant coefficients of the sixth-degree polynomial function, previously proposed by us, have been found. In result of this there were obtained two analytic equations of vehicles' movement, where one of them presented with the positive sign of the leading coefficient and the other one negative. These two equations allowed to make comprehensive investigation of the delays and the kinematics of the vehicles moving by such kinds of lanes. Based on the appropriate calculations it is determined vehicles' consequent delays, velocities, accelerations and decelerations. Analyzing the delays, the dynamics of accelerations and decelerations, it is done an assumption that if the leading coefficient of algorithm of movement of vehicles is negative than it will lead to larger deceleration and consequently higher environmental pollutions and higher noises.

Keywords

Hypothetical, Statistical, Simulation, Movement, Acceleration, Deceleration, Delay, Pollution, Noise, Harsh

1. Introduction

A hypothetical-statistical model for vehicles dynamics was first developed in the traffic flow simulation program VISSIM ("VerkehrInStädten—SIMulationsmodell"; German for "Traffic in cities—simulation model"). VISSIM to study the general operational effect of the additional lane. Then a hypothetical double lane roundabout with four legs was first examined in VISSIM under varying additional lane lengths at the entry and exit. Findings from the hypothetical-statistical model are then compared with that of an existing roundabout. For comparison purposes, similar variations were then tested on an existing double lane roundabout with data from NCHRP 572. The Brattleboro roundabout in Vermont has been used for consideration. It is a double lane roundabout with four legs aligned at 90 degrees. This is one of the roundabouts that the NCHRP 572 collected data on to study the roundabout operations in the United States. The data from the NCHRP 572 study is used to calibrate and validate the model in VISSIM. The Brattleboro roundabout has similar configuration to the hypothetical-statistical model used some studies. Analyses of both the hypothetical-statistical and existing roundabout models indicated that very long additional lane lengths were not effective in reducing delay at roundabouts. Shorter lengths up to 150 feet were demonstrated to be most effective. This finding corresponds to the results from the U.K. Department of Transportation *Design Manual Road and Bridges,* which recommended shorter flare lengths of about 82 feet to effectively increase capacity and pointed out that larger flare resulted in higher speeds.

Authors of the works [1] [2] [3] give very detail description about application of the hypothetical-statistical model for roundabout designing and analyzing. It is shown that through the analyses of both hypothetical and existing roundabout models, there are diminishing returns on reduction of overall delay as the additional length increases or there are distinct distances where one sees less change per additional increase in the approach length. Based on the hypothetical-statistical models here it is considered such important properties and characteristics of roundabouts traffics and design as: entry flow (vhe/hr); turning movements; entry volume lane distributions (veh/hr); critical lane capacity (pc/h); volume-to-capacity ratio (V/C); initial simulation delay data; descriptive statistics; double lane roundabout model development and analyzing; travel time; data queue lengths; VISSIM output results and entire roundabout intersection delay data. For the research effort, using the delay as the measure of effectiveness, two roundabout situations are modeled and analyzed extensively. One is a hypothetical four-leg, double-lane roundabout with additional lane design at both entry and exit approaches. In this research the geometric guidelines from the NCHRP Report 672 were used in setting up the hypothetical-statistical model. Here it is presented initial VISSIM simulation data for hypothetical and existing models before calibration. Due to the lack of validated analytical models, the hypothetical-statistical model was analyzed using VISSIM default values with average of the measure of effectiveness calculated within an acceptable level of 30% confidence. For the hypothetical-statistical model, VISSIM default values for headway were used. Data collection points used for capturing delay data in VISSIM for the hypothetical-statistical model were placed at similar locations specified in the NCHRP 572 so as to be able to compare results.

2. Literature Review

In the paper [4] authors have considered hypothetical-statistical model in conception of determination the time in Quantum Mechanics. In this work it takes place discussion of a hypothetical-statistical interpretation of the dwell time in terms of individual members of the ensemble, and the dwell time is at the very least a characteristic quantity of the ensemble represented by the special function that quantifies the duration of the wave packet collision. Bio-verse as a simulation framework to assess the statistical power of future biosignature surveys is presented in the publication [5]. Bio-verse combines existing knowledge of exoplanet statistics with a survey simulation and hypothesis testing framework to determine whether proposed space-based direct imaging and transit spectroscopy surveys will be capable of detecting various hypothetical-statistical relationships between the properties of terrestrial exoplanets. The purpose of the paper [6] is to examine how usage of a statistical power analysis can improve researcher's decision about choosing an appropriate sample size for experimental purposes and quality inspection. Observation through a hypothetical-statistical example based on a significance test in which the difference between proportions of two independent samples was estimated. The research work [7] is aimed at the design of a pipeline leakage detection system. Of the hardware-based detecting methods is the use of acoustics, fiber optics, ultrasonics, infrared radiometrics, vapour or liquid sensing tubes, and cable sensors, while mass/volume balance, transient modeling, hypothetical-statistical analysis, and pressure analysis are examples of software-based methods. Authors of the paper [8] experimentally investigated the dynamic behavior of the combustion instability in a lean premixed gas-turbine combustor from the viewpoint of nonlinear dynamics. They indicated that applying the nonlinear time series analysis to the analysis of experimental data, a surrogate data method known as a hypothetical-statistical test has been introduced as an effective method of validating the nonlinear determinism in complex dynamic behavior deduced. Authors of the work [9] dedicated they investigation to the Mathematical Research regarding to testing statistical hypotheses, considered so called one, two and multi-sides hypotheses as well as linear, equivalence and approximate hypotheses. In the work [10] the hypothetical-statistical model shows that unless the database of episodes involved in testing the success of the add-on dual chamber detection features is identical for the different devices. In order to illustrate the most common forms of non-independence related to island biogeography authors of the paper [11] explore a hypothetical-statistical model that aims to address island area as a predictor of the species richness of ten distinct taxa across all of the islands. In the paper [12] it is stated that speckle (image of a small spot) filtering is achieved by making the histogram of a homogeneous region fit the distribution function of a prior hypothetical-statistical model as much as possible. The authors of the investigation [13] presented the hypotheses for the GOF (Goodness-of-Fit for) test. It is noted that the proposition that the hypothetical-statistical model fits the observed distribution is equivalent to fail to reject null hypothesis (the statement assumed to be true). In the research [14] [15] the proposed method of investigation is presented in the Bayesian framework. In this works from a hypothetical-statistical model for the image, a gain estimator is from a theoretical basis. Authors of the paper [16] notedthe developed techniques for drawing the inference from time series. One of the primary goals of time series analysis is to set up a hypothetical-statistical model to represent the series in order to obtain insights into mechanism that generate the data. The investigator of the publication [17] indicates that the shortcomings in the methodology of statistical-hypothesis testing used in educational and psychological research have been emphasized repeatedly, and the hypothesis testing is a central and complex problem in the methodology of science. Author of this paper remarked that theories are not substantiated by the goodness of fit between the data and a hypothetical-statistical model but rather by the estimation of significant parameters in the statistical model. In the paper [18] it is considered the probabilistic aspects of the actual experimental process itself and derivation of the hypothetical-statistical model. The researchers of the papers [19] [20] [21], dedicated to theparallel evolution simulation model of algorithm of dust particles in campus environment, indicated that the basic idea of the Monte-Carlo method is that the solution of the problem is equivalent to a hypothetical-statistical model parameter which can be calculated by using random number, and the parameters are estimated by the statistical model of a testing sample. The paper [22] is proposed a spectrum sensing algorithm based on a deep learning convolutional neural network, which avoided the influence of the accuracy of the hypothetical-statistical model on the detection results and improved the detection probability. The researchers of the work [23] noted that Eco-Driving, a driver behavior-based method, has featured in a number of national policy documents as part of CO_2 emissions reduction or climate change strategies. This investigation comprises a detailed assessment of acceleration and deceleration in Eco-Driving Vehicles at different penetration levels in the vehicle fleet, under varying traffic composition and volume. The impacts of Eco-Driving on network-wide traffic and environmental performance at a number of speed restricted road networks (30km/hr) is quantified using Micro-simulation. The results show that increasing levels of Eco-driving in certain road networks results in significant environmental and traffic congestion detriments at road network level in the presence of heavy traffic. Increases in CO_2 emissions of up to 18% were found. However, with the addition of vehicle-to-vehicle or vehicle-to-infrastructure communication technology which facilitates dynamic driving control on speed and acceleration/deceleration in vehicles, improvements in CO_2 emissions and traffic congestion are possible using Eco-Driving. Authors of the paper [24] examine the effects of varying key roundabout parameters within the SimTraffic and VISSIM microsimulation models by analyzing predicted operations for a hypothetical roundabout under three volume scenarios. The paper [25] introduced the simulation of a hypothetical roundabout corridor on Wanamaker Road in Topeka, KS using SIDRA and VISSIM showed significant reductions in delay and queueing for most all significant traffic movements. In the work [26] it is shown a figure which represents a hypothetical roundabout layout based on real roundabout dimensions that portrays potential differences in speed between a smaller curvilinear exit and a more tangential exit. Here it is noted that the two research projects discussed both used uniform acceleration in their calculations. The acceleration rate chosen for design will also have an effect on the predicted speed. From their observations and analysis, the authors developed equations that, in some locations, may better predict entry and exit speeds based on vehicle deceleration and acceleration ability. In the publication [27] the output resulting from the simulations of the both the existing intersections on Wanamaker at Huntoon and the I-470 off-ramp and the hypothetical roundabout on Wanamaker at Huntoon and the I-470 off-ramp with right turns only are summarized in a table. The average delay for all approaches at Wanamaker is reduced from 32.8 seconds to 9.5 seconds for the hypothetical roundabout as compared to the current signalized intersection. In some certain section of the paper [28] two simulation experiments were conducted based on a hypothetical roundabout. Experiment 1 was to test the effectiveness of multi-level traffic control (MTC) and the experiment 2 was to verify the operational advantage of MTC over yield control and fully actuated control. The purpose of the study [29] was to examine a sample of signalized intersections in Northern Virginia that were newly constructed or recently underwent major modifications and to determine the extent to which hypothetical roundabouts could have affected traffic flow and safety. Standard operational measures of intersection performance were computed for the locations operating under traffic signal control and then compared with values estimated for the same intersections operating with hypothetical roundabouts. Hypothetical roundabouts were designed so as to roughly match the vehicle capacity provided by the existing signalized intersections. Here the vehicle delay was the principal operational measure chosen to define traffic congestion. The table developed in this work compares average vehicle delays for the ten signalized intersections with those for the same locations using hypothetical roundabouts. The paper [30] referred about a hypothetical roundabout (7m diameter) generated in Rhinoceros V5.0 modeling tool and placed centrally in the original reconstruction of the crash site. Here the vehicles speed was gradually decreased, and steering inputs varied until the vehicles were able to navigate through the roundabout. The crash was simulated at the highest speed at which the case and B-vehicle (motorcycles, trucks, vans, buses, etc.) could navigate through the roundabout. The underlying approach in thesis [31] involves the simulation of hypothetical roundabout networks and intersection networks with varying complexity and comparison of performance using statistical methods. The authors of the final report [32] analyzed a hypothetical four-leg, double-lane roundabout with additional lanes at both entry and exit. They varied the lengths of these additional lanes to study their effect on operations. Based on the findings from the hypothetical roundabout, similar additional lane lengths were applied to a calibrated and validated model of an existing roundabout. The findings indicate that shorter lengths of additional lanes (and flares) of 50 to 150 feet provided the best operational performance. Author of the paper [33] noted that numerous studies showed that the application of modern roundabouts can help reduce the excessive emissions and fuel consumption and noise pollution associated with idling time, acceleration and deceleration of vehicles that usually occur on traditional signalized intersections, which is particularly important for urban environments. The acceleration and deceleration of vehicles are considered from the beginning of the entry lane of roundabouts up to vehicles' totally exit from roundabouts. In the paper [34] drive cycles are defined by the initial and final speeds in each element of the driving maneuver. The drive cycle information is used to calculate acceleration and deceleration times and distances for each element of the drive cycle individually. The fuel consumption, emission rates and operating cost values are calculated for each element of the drive cycle individually and the results are added together for the entire queued vehicle maneuver, and then the results for queued and unqueued vehicles are aggregated. The investigators of the paper [35] indicated that numerous researchers have linked the geometric parameters of roundabouts to important aspects of roundabout design including speed and safety performance. There is also evidence that good geometric design of roundabouts as well as their entry and exit lanes can improve environmental sustainability. The model was applied to a hypothetical example to test its ability to determine the optimal geometric parameters. The results revealed that the model identified the geometric parameters that minimize vehicle emissions. A sensitivity analysis was conducted and revealed that using the optimal geometric parameters provided by the model improved the environmental sustainability of the roundabout. The use of the model resulted in reductions of 10.7%, 25%, 6%, and 31% for NOX, HC, CO_2, and CO emissions (respectively) compared to increasing the optimal geometric parameters by 5%. In this study, the acceleration and deceleration rates were assumed to be constant for emissions calculations, as recommended by the guidelines. The analysis in the paper [36] suggests that, with the addition of checks for available deceleration and acceleration, the current FHW guidelines for predicting speed and speed differences are adequate. The high predicted entry speeds that resulted from the small deflection at the entries were reflected in the observed speeds at the roundabouts. The researchers of the paper [37] considered that congestion is deemed to be a significant source of vehicle emissions, because stop-and-go traffic and associated acceleration/deceleration patterns have been linked to increased emissions. Roundabouts can have operational and safety benefits over signalized intersections under certain circumstances. For example, the average vehicle delay can be significantly lower during off-peak periods for roundabouts compared to signalized intersections, and under peak traffic conditions, roundabouts can often match or even outperform traffic signals operationally. Due to the geometric and design characteristics of roundabouts, they can function as a traffic calming device, and they have been shown to provide substantial safety benefits over signalized intersections. However, it is noted that the accelerations lead to high fuel use rates compared to idling or deceleration. In the work [38] it is indicated the followings: roundabouts can provide environmental benefits if they reduce vehicle delay and the number and duration of stops compared with an alternative. Even when there are heavy volumes, vehicles continue to advance slowly in moving queues rather than coming to a complete stop. This may reduce noise and air quality impacts and fuel consumption significantly by reducing the number of acceleration/deceleration cycles and the time spent idling. Authors of the work [39] noted that high vehicle acceleration and deceleration values, driving brake, different obstacles that cause traffic queues and a high traffic flow at the area are some of the issues that increase the risk of traffic noise. Some investigations show that increase/decrease in noise level caused by varying levels of acceleration/deceleration and different vehicle types with speed of 50 km/h. The contributions of the paper [40] are 1) the formulation of the problem of controlling automated vehicles before they enter a roundabout at a lower speed, 2) implementing an analytical solution that yields the optimal acceleration/deceleration for each vehicle, and 3) the investigation of the optimal solution through simulation under different traffic conditions. Considering the presence of automated vehicle technologies, the maximum acceleration and the minimum deceleration are set to 4.5 m/s^2 and −4.5 m/s^2, respectively. Authors of research [41] investigated the method of calculation of delay due to additional entry lane of roundabout. For that here it is proposed to represent the kinematic of movement of the vehicles through the additional lane as 6^{th} degree polynomial function. In the work [42] it is stated that in real-world conditions there are driving areas where the traffic flow is uneven, taking place braking, acceleration, deceleration and stopping. These circumstances entail an increase in the amount of pollutants from vehicles. The main effect on both fuel consumption and emissions of toxic substances is exerted by the acceleration and deceleration modes. To take into account the effect of acceleration and deceleration rates on automobile emissions of pollutants, it is proposed to use correction factors, taking into account the effect of acceleration intensity on the emission of pollutants; mileage emission of the i^{th} pollutant in acceleration and deceleration modes to the certain speed, etc. The total mass emission of pollutants on a simulated section of the traffic way by one passenger car for carbon monoxide (CO) and nitrogen oxides (NOx) have calculated. In the [43] a model is developed by considering speed as the factor for vehicular emissions. A model is proposed to estimate the emission factor for CO_2 emissions, considering speed as the predictor variable using the on-board emission measurement data. Here it is discussed the effect of acceleration and deceleration, and cruise modes on the emission rates at various speeds. The on-board emission measurement includes the effect of the acceleration and deceleration in estimating the emission rates for various speeds. To demonstrate the effect of the acceleration and deceleration on the emission rates, first a discussion on how the fuel consumption is affected by acceleration and deceleration.

Here it is introduced the effect of acceleration and deceleration on speeds with respect to time and the resulting fuel consumption for different driving modes. In an analysis that was performed to study the effect of the accelerations and decelerations on the emission rates, it was determined that at higher speeds, small fluctuations in speed would significantly affect the emission rates. In the method, proposed by authors of [44] the vehicle noise responds to the vehicle type, speed, environmental effect corrections and acceleration/deceleration. In contexts with this here it is noted that vehicles' accelerations and decelerations leading to an effect in the noise emission. It is shown that comparing crossing and roundabout intersections, the sound power level distribution from the whole road traffic network is very similar in both situations, increasing its percentage in the lower ranges in the case of the roundabout. If acceleration and deceleration are removed, the range spread is reduced and condensed mainly in the range of 85 dBA (around 70% for signalized crossing and 73% for roundabout), where both higher and lower ranges are reduced. Researchers of the paper [45] shows that the rationale behind the claim of lowering (air pollutant) emissions is that congestion causes vehicles to function at sub-optimal speeds and accelerations, leading to incomplete combustion and additional emissions of NO_x, CO, etc. For heavy duty vehicles, acceleration has a more pronounced effect on noise emission, which is not the case for light duty vehicles, due to the engine noise being more controlled. Her significant effects of congestion on emission are indicated. The report [46] stated that for vehicles moving at very low speeds, repeated acceleration and deceleration movements cause high emissions rates per vehicle per mile. At high speeds (*i.e.*, above 60 mph), emissions rates increase because aerodynamic resistance places increasing demands on engine power. This non-linear relationship between emissions rates and speed suggests two important factors that affect the emissions impacts of daytime versus nighttime construction. The study [47] says that acceleration and deceleration plays the most crucial role in emissions from motor vehicles. For quantifying the impact of each of the driving profiles on traffic and emissions, the acceleration and deceleration values of the *dau*, *hrs*, and *eco* profiles were introduced to the Krauss model [48]. The impact of acceleration and deceleration ranges on the environment can be assessed by plotting the CO_2 emissions per vehicle per kilometer in relationship to the traffic density. As can be observed, profile *eco* results in the lowest emissions of CO_2 justifying the assumption that lower values of acceleration and deceleration lead to lower fuel consumption. It has been shown that placing a limit on the acceleration and deceleration characteristics of vehicles has a positive impact both on the properties of traffic flow and the emission of harmful air pollutants. A notable improvement could be acceleration and deceleration profiles relative to the speed levels, because, in typical passenger cars, a vehicle is capable of higher accelerations in lower speeds and lower accelerations in higher speeds. The objective of the study [49] is to develop emissions models which can incorporate acceleration or deceleration. This study developed analytical emissions models that can be integrated with existing microscopic traffic models for project evaluation. Due to the difficulty in representing acceleration or deceleration in macroscale emissions models, microscale emissions models were developed that can estimate second-by-second emissions for given variables such as acceleration or deceleration and speed at the current and previous time periods. In the investigation [50] the authors referred to the fact that all scenarios in one way or another, attempted to suppress shockwaves, which resulted in travel time improvements, increased safety through reduction of speed variation and sudden changes in acceleration/deceleration, which in turn lessened fuel consumption and emissions. These traffic perturbations result in higher acceleration/deceleration which burns 20%-30% more fuel and CO_2 emission. The paper [47] assesses the impact of adopting smooth driving habits on traffic and emissions in large scale urban networks. Here an integrated data driven and simulation methodology is proposed, which, first tries to reveal the prevailing driving profiles using real world driving behavior data gathered from smartphones, and second, to simulate the effect of controlling the observed profiles on traffic and emissions using microscopic simulation. The simulation results show that smooth driving leads to a statistically significant reduction in the emissions of the most important air pollutants. It is suggested that the impact of acceleration and deceleration ranges on the environment can be assessed by plotting the CO_2 emissions per vehicle per kilometer in relationship to the traffic density. It is also worth noting that driving force-running resistance balance diagram is well discussed in the research of vehicle dynamics [51]. In the work [52] it has been proposed a microscopic model to traffic flow that adds to the understanding of the different types of congestion that are found in traffic flow. The main assumption the model is based on is the fact that in general vehicles move without colliding. The model is mainly characterized by the parameters describing typical acceleration and deceleration capabilities of the vehicles. By varying acceleration and deceleration capabilities a thorough understanding of the dynamics of the model and the previously known special cases is gained. In a summary, this research is aimed to study the delays, the dynamics of accelerations and decelerations when an additional entry lane is used for a roundabout. The research will also look into an optimal length to enhance operations with an implication of lower speed on the approach.

3. Calculations

Calculation of the delay due to the entry lane of the roundabouts is the measure of effectiveness used in this study. For calculations it is assumed that the length of the additional second entry lane of the roundabout and the speed of the vehicles, entering that line, are given. Here data collections and calculations are performed for the length L of the additional lane about 430 ft and the initial velocity V_0 of the vehicles (entering that lane) around 25 MPH. Therefore, in created **Tables 1-3**, shown below the velocities are given in MPH, and the distances in ft. These tables have been generated on the base of the well-known hypothetical-statistical method having wide applications in different fields of human activities, such as in the Applied Engineering Mathematics, Statistics, Physics, Combustion Science and Technology, Computer Sciences. Medicine, Biogeography, Imaging Processing, Satellite, Space Biology, Educational and Psychological, etc. Application of the hypothetic statistic method is able to reflect the real operation performance of the roundabouts, included their entrances and exits. Based on this method we provide implementation of development of the models of simulation the observing traffic. Thus, all of numbers in **Tables 1-3** formed on the base of the hypothetical-statistical model of the traffic flowing data. These simulated models will allow pre-analysis some significant parameters of traffic, such us optimal length of the additional lane, delays, etc. Also, it will able to predict density, speed, and delay for each time slice within the analytical period (which can be longer than an hour). Here we use precise and simple way of estimation of the delay, based on our previously proposed and developed method. As it shown in our publication [41] this analytic method applying constant coefficients of the sixth-degree polynomial function allows to calculate that important parameter of traffic ease and rapid with very high accuracy. Using delay as the measure of effectiveness, here a hypothetical four-leg roundabout with additional entry is analyzed. It should be mentioned that usually the additional lane lengths are varied at both entry and exit and this circumstance demonstrates the effect of different additional lane lengths on roundabout operation. However, Dr. Samuel Hammond in his Dissertation Research [1] very detail described that circumstance in practice: it is indicated that very long additional lane lengths ($250 \text{ ft} \le L \le 550 \text{ ft}$) result in higher speeds on the approach but were not necessarily providing the greatest overall impact in reducing delay through the roundabout. So, here the main goal is to determine the operational impact of additional lane length and queue length in roundabouts and quantify the reduction of delay and travel time. Our practical calculations below are intended to provide transportation professionals quantitative means of improving existing roundabout operational performance. It should aid during the planning and design stage and also to help to develop and to build future roundabouts with appropriate additional lane lengths that yield better results. However, it is very important to note that because here we very often use hypothetical-statistical data, then on the base of this circumstance we just want to show the rightfulness of the conception of our proposed method of calculation of the delays. Based on this condition, in order to make our further calculations simple, easy and clear, we are proposing to show some numbers in Tables, representing the coordinates, lengths and speeds, as the whole numbers. Because here the considered time intervals are very low, so all of time factors will be rounded up to second decimals. All of our calculations are done with the consideration of the case when traffic takes place right at the rush hour time. It is assumed that observation time is around 15min. Regarding to all these circumstances below are shown Tables from 1 to 3 created by the applied hypothetical-statistical

Table 1. Vehicle speed and travel distance for the additional lane length of 250 ft.

Detected vehicles number	1	2	3	4	5	6	7	8	9	10	11	12	13	14	15
Their maximum speeds $V_{\max_i}$	36	37	35	38	36	34	32	39	35	34	37	36	33	38	40
Coordinates $S_{\max_i}$ of $V_{\max_i}$	124	130	129	126	131	127	128	125	128	135	126	133	124	132	131
Coefficient C_i	1.44	1.48	1.40	1.52	1.44	1.36	1.28	1.56	1.40	1.36	1.48	1.44	1.32	1.52	1.60
Coefficient q_i	0.29	0.30	0.30	0.29	0.31	0.29	0.30	0.29	0.30	0.31	0.29	0.31	0.29	0.31	0.30

Detected vehicles number	16	17	18	19	20	21	22	23	24	25	26	27	28	29	30
Their maximum speeds $V_{\max_i}$	33	36	36	32	38	37	35	34	42	33	36	39	35	34	36
Coordinates $S_{\max_i}$ of $V_{\max_i}$	131	125	127	129	130	132	126	129	129	125	127	133	129	128	129
Coefficient C_i	1.32	1.44	1.44	1.28	1.52	1.48	1.40	1.36	1.68	1.32	1.44	1.56	1.40	1.36	1.44
Coefficient q_i	0.31	0.29	0.29	0.30	0.30	0.31	0.29	0.30	0.30	0.29	0.29	0.31	0.30	0.30	0.30

Detected vehicles number	31	32	33	34	35	36	37	38	39	41	41	42	43	44	45
Their maximum speeds $V_{\max_i}$	40	33	36	35	31	38	37	34	39	32	35	40	36	33	35
Coordinates $S_{\max_i}$ of $V_{\max_i}$	126	124	127	128	132	130	134	126	128	125	123	131	127	129	133
Coefficient C_i	1.60	1.32	1.44	1.40	1.24	1.52	1.48	1.36	1.56	1.28	1.40	1.60	1.44	1.32	1.40
Coefficient q_i	0.29	0.29	0.29	0.30	0.31	0.30	0.31	0.29	0.30	0.29	0.29	0.31	0.29	0.30	0.31

Detected vehicles number	46	47	48	49	50	51	52	53	54	55	56	57	58	59	60
Their maximum speeds $V_{\max_i}$	33	37	35	38	40	39	34	36	42	38	34	37	39	41	32
Coordinates $S_{\max_i}$ of $V_{\max_i}$	129	134	130	128	131	133	129	126	127	132	127	125	131	126	125
Coefficient C_i	1.32	1.48	1.40	1.52	1.60	1.56	1.36	1.44	1.68	1.52	1.36	1.48	1.56	1.64	1.28
Coefficient q_i	0.30	0.31	0.30	0.30	0.31	0.31	0.30	0.29	0.29	0.31	0.29	0.29	0.30	0.29	0.29

Detected vehicles number	61	62	63	64	65	66	67	68	69	70	71	72	73	74	75
Their maximum speeds $V_{\max_i}$	35	36	34	42	38	37	32	39	40	31	39	34	35	36	39
Coordinates $S_{\max_i}$ of $V_{\max_i}$	128	132	129	127	126	124	130	133	129	125	131	127	128	126	130
Coefficient C_i	1.40	1.44	1.36	1.68	1.52	1.48	1.28	1.56	1.60	1.24	1.56	1.36	1.40	1.44	1.56
Coefficient q_i	0.30	0.31	0.30	0.29	0.29	0.29	0.30	0.31	0.30	0.29	0.30	0.29	0.30	0.29	0.31

Detected vehicles number	76	77	78	79	80	81	82	83	84	85	86	87	88	89	90
Their maximum speeds $V_{\max_i}$	37	32	35	38	36	40	42	37	39	34	33	38	32	37	35
Coordinates $S_{\max_i}$ of $V_{\max_i}$	131	129	123	132	128	125	126	124	133	131	127	124	130	129	127
Coefficient C_i	1.48	1.28	1.40	1.52	1.44	1.60	1.68	1.48	1.56	1.36	1.32	1.52	1.28	1.48	1.40
Coefficient q_i	0.30	0.30	0.29	0.31	0.30	0.29	0.29	0.29	0.31	0.30	0.29	0.29	0.30	0.30	0.29

Table 2. Vehicle speed and travel distance for the additional lane length of 400 ft.

Detected vehicles number	**1**	**2**	**3**	**4**	**5**	**6**	**7**	**8**	**9**	**10**	**11**	**12**	**13**	**14**	**15**
Their speeds V_{0_i} around of V_0	27	24	26	28	25	30	27	29	22	24	26	25	23	25	28
Coordinates S_{0_i} of those speeds	254	248	245	245	255	249	251	245	243	252	256	247	252	254	250
Coefficient h_i	1.08	0.96	1.04	1.12	1.00	1.20	1.08	1.16	0.88	0.96	1.04	1.00	0.92	1.00	1.12
Coefficient v_i	0.59	0,58	0.57	0.57	0.59	0.58	0.58	0.57	0.57	0.59	0.60	0.57	0.59	0.59	0.58

Detected vehicles number	**16**	**17**	**18**	**19**	**20**	**21**	**22**	**23**	**24**	**25**	**26**	**27**	**28**	**29**	**30**
Their speeds V_{0_i} around of V_0	23	26	26	27	28	24	25	24	27	29	26	30	25	24	26
Coordinates S_{0_i} of those speeds	251	255	257	249	250	252	256	248	249	258	247	249	250	254	252
Coefficient h_i	0.92	1.04	1.04	1.08	1.00	1.20	1.08	0.96	1.08	1.16	1.04	1.20	1.00	0.96	1.04
Coefficient v_i	0.58	0.59	0.60	0.58	0.58	0.59	0.60	0.58	0.59	0.60	0.57	0.58	0.58	0.59	0.59

Detected vehicles number	**31**	**32**	**33**	**34**	**35**	**36**	**37**	**38**	**39**	**41**	**41**	**42**	**43**	**44**	**45**
Their speeds V_{0_i} around of V_0	29	23	26	25	24	28	27	24	23	26	25	26	24	30	22
Coordinates S_{0_i} of those speeds	255	250	251	249	254	257	252	256	250	258	247	249	251	250	254
Coefficient h_i	1.16	0.92	1.04	1,00	0.96	1.12	1.08	0.96	0.92	1.04	1.00	1.04	0.96	1.20	0.88
Coefficient v_i	0.59	0.58	0.58	0.58	0.59	0.60	0.59	0.60	0.58	0.60	0.57	0.58	0.58	0.58	0.59

Detected vehicles number	**46**	**47**	**48**	**49**	**50**	**51**	**52**	**53**	**54**	**55**	**56**	**57**	**58**	**59**	**60**
Their speeds V_{0_i} around of V_0	28	24	26	29	22	25	23	27	25	28	24	26	28	30	25
Coordinates S_{0_i} of those speeds	256	252	250	247	249	251	258	250	253	255	251	259	247	251	253
Coefficient h_i	1.12	0.96	1.04	1.16	0.88	1.00	0.92	1.08	1.00	1,12	0.96	1.04	1.12	1.20	1.00
Coefficient v_i	0.60	0.59	0.58	0.57	0.58	0.58	0.60	0.58	0.59	0.59	0.58	0.60	0.57	0.58	0.59

Detected vehicles number	**61**	**62**	**63**	**64**	**65**	**66**	**67**	**68**	**69**	**70**	**71**	**72**	**73**	**74**	**75**
Their speeds V_{0_i} around of V_0	25	27	29	24	22	26	23	28	25	27	28	30	22	24	25
Coordinates S_{0_i} of those speeds	253	255	251	248	252	249	250	253	259	246	248	247	250	252	256
Coefficient h_i	1.00	1.08	1.16	0.96	0.88	1.04	0.92	1.12	1.00	1.08	1.12	1.20	0.88	0.96	1.00
Coefficient v_i	0.59	0.59	0.58	0.58	0.59	0.58	0.58	0.59	0.60	0.57	0.58	0.57	0.58	0.59	0.60

Detected vehicles number	**76**	**77**	**78**	**79**	**80**	**81**	**82**	**83**	**84**	**85**	**86**	**87**	**88**	**89**	**90**
Their speeds V_{0_i} around of V_0	26	23	27	25	24	27	22	29	30	25	29	28	26	23	27
Coordinates S_{0_i} of those speeds	250	254	249	251	248	252	255	258	259	247	246	250	253	255	246
Coefficient h_i	1.04	0.92	1.08	1.00	0.96	1.08	0.88	1.16	1.20	1.00	1.16	1.12	1.04	0.92	1.08
Coefficient v_i	0.58	0.59	0.58	0.58	0.58	0.59	0.59	0.60	0.60	0.57	0.57	0.58	0.59	0.59	0.57

Table 3. Vehicle speed and travel distance for the additional lane length of 550 ft.

Detected vehicles number	**1**	**2**	**3**	**4**	**5**	**6**	**7**	**8**	**9**	**10**	**11**	**12**	**13**	**14**	**15**
Their minimum speeds $V_{\min_i}=0$	0	0	0	0	0	0	0	0	0	0	0	0	0	0	0
Coordinates $S_{\min_i}$ of speeds $V_{\min_i}$	348	350	346	351	349	350	352	353	346	345	347	344	352	354	341
Coefficient r_i	0.81	0.81	0.81	0.82	0.81	0.81	0.82	0.82	0.81	0.80	0.81	0.80	0.82	0.82	0.79

Detected vehicles number	**16**	**17**	**18**	**19**	**20**	**21**	**22**	**23**	**24**	**25**	**26**	**27**	**28**	**29**	**30**
Their minimum speeds $V_{\min_i}=0$	0	0	0	0	0	0	0	0	0	0	0	0	0	0	0
Coordinates $S_{\min_i}$ of speeds $V_{\min_i}$	351	355	349	350	344	346	347	350	348	345	353	340	356	349	352
Coefficient r_i	0.82	0.83	0.81	0.81	0.80	0.81	0.81	0.81	0.81	0.80	0.82	0.79	0.83	0.81	0.82

Detected vehicles number	**31**	**32**	**33**	**34**	**35**	**36**	**37**	**38**	**39**	**41**	**41**	**42**	**43**	**44**	**45**
Their minimum speeds $V_{\min_i}=0$	0	0	0	0	0	0	0	0	0	0	0	0	0	0	0
Coordinates $S_{\min_i}$ of speed $V_{\min_i}$	345	354	341	347	350	344	348	351	352	349	343	348	356	357	344
Coefficient r_i	0.80	0.82	0.79	0.81	0.81	0.80	0.81	0.82	0.82	0.81	0.80	0.81	0.83	0.83	0.80

Detected vehicles number	**46**	**47**	**48**	**49**	**50**	**51**	**52**	**53**	**54**	**55**	**56**	**57**	**58**	**59**	**60**
Their minimum speeds $V_{\min_i}=0$	0	0	0	0	0	0	0	0	0	0	0	0	0	0	0
Coordinates $S_{\min_i}$ of speed $V_{\min_i}$	352	349	345	351	355	344	342	353	348	347	350	352	354	340	341
Coefficient r_i	0.82	0.81	0.80	0.82	0.83	0.80	0.80	0.82	0.81	0.81	0.81	0.82	0.82	0.79	0.79

Detected vehicles number	**61**	**62**	**63**	**64**	**65**	**66**	**67**	**68**	**69**	**70**	**71**	**72**	**73**	**74**	**75**
Their minimum speeds $V_{\min_i}=0$	0	0	0	0	0	0	0	0	0	0	0	0	0	0	0
Coordinates $S_{\min_i}$ of speed $V_{\min_i}$	347	340	358	349	352	344	355	346	351	352	344	348	350	343	349
Coefficient r_i	0.81	0.79	0.83	0.81	0.82	0.80	0.83	0.81	0.82	0.82	0.80	0.81	0.81	0.80	0.81

Detected vehicles number	**76**	**77**	**78**	**79**	**80**	**81**	**82**	**83**	**84**	**85**	**86**	**87**	**88**	**89**	**90**
Their minimum speeds $V_{\min_i}=0$	0	0	0	0	0	0	0	0	0	0	0	0	0	0	0
Coordinates $S_{\min_i}$ of speed $V_{\min_i}$	353	341	348	351	355	340	357	344	352	347	345	357	349	353	354
Coefficient r_i	0.82	0.79	0.81	0.82	0.83	0.79	0.83	0.80	0.82	0.81	0.80	0.83	0.81	0.82	0.82

approach and simulation runs data.

Based on the above obtained formulas and the data, collected in these three tables, here such parameters have been calculated as velocities and distances $V_{\max}$, $S_{\max}$, $V_{\max}^{avg}$, $S_{\max}^{avg}$, $S_{\min}$ as well as coefficients *q*, *r v*, *v*, *c* and *h*. Our calculations are based on the assumption that the number of the observed vehicles in the traffic is $n=90$. In our publication [41] we obtained the mathematical algorithm $V(s)$ represented the kinematics of movement of the vehicles through the additional entry lanes of the roundabouts. It is introduced as the sixth-degree polynomial function, depended on from the way S currently covered by the given vehicle. So, the speed of the vehicles $V(s)$ as well as their accelerations $a(s)=\frac{\mathrm{d}V(s)}{\mathrm{d}s}>0$ and decelerations $-a(s)=\frac{\mathrm{d}V(s)}{\mathrm{d}s}<0$ with respect to distance Scan be presented consequently as the sixth and fifth degree nonlinear polynomial functions, that is:

$$V(s)=AS^6+BS^5+CS^4+DS^3+ES^2+V_0 \tag{1}$$

$$a(s)=\frac{\mathrm{d}V(S)}{\mathrm{d}S}=S\cdot\left(6AS^4+5BS^3+4CS^2+3DS+2E\right) \tag{2}$$

As it described in our publication for derivation of the sixth-degree polynomial function $V(s)$ there have to be determined the values of the constants *A, B, C, D* and *E*. For that porpoise here have to be considered the conditions, related to the movements of the vehicles. Because the graph of our proposed function $V(s)$ must have just a maximum and two minimum points [41], therefore, on the base of these circumstances here it is required to find the following five conditions for determination the final form of the function $V(s)$: 1) the maximum value of velocity and its consequent coordinate ($V_{\max}^{sm}$; $S_{\max}^{sm}$), 2) the first derivative of function, that is acceleration, at the same point $\left[\frac{\mathrm{d}V(s)}{\mathrm{d}s}=0;S_{\mathrm{ma}}^{sm}\right]$, 3) the coordinate of function ($S\neq 0$) when velocity of vehicle again equal to its initial velocity $\left(V_0;S_0^{sm}\right)$, 4) the minimum point of function when its value equal to zero $\left[V(s)=0;S_{\min}\right]$, 5) the first derivative of function, that is deceleration, at the same point $\left[\frac{\mathrm{d}V(s)}{\mathrm{d}s}=0;S_{\min}\right]$. All of these coordinates are found from the above tables developed based on hypothetical-statistical models and simulation of the kinematics of vehicles' movement. Below are the calculated values all of those coordinates.

The results of calculations based on the data of the Table 1

$$\text{(a)}\quad V_{\max}^{sm}=\frac{\sum_{i=1}^{i=90}V_{\max_i}\cdot S_{\max_i}}{\sum_{i=1}^{i=90}S_{\max_i}}=\frac{418360\text{ MPH}\cdot\text{ft}}{11558\text{ ft}}\approx 36.2\text{ MPH},$$

$$\text{(b)}\quad V_{\max}^{avg}=\frac{\sum_{i=1}^{i=90}V_{\max_i}}{90}=\frac{3257\text{ MPH}}{90}\approx 36.2\text{ MPH}, \tag{3a,b}$$

$$\text{(a)}\quad S_{\max}^{sm}=\frac{\sum_{i=1}^{i=90}V_{\max_i}\cdot S_{\max_i}}{\sum_{i=1}^{i=90}V_{\max_i}}=\frac{418360\text{ MPH}\cdot\text{ft}}{3257\text{ MPH}}\approx 128.5\text{ ft},$$

$$\text{(b)}\quad S_{\max}^{avg}=\frac{\sum_{i=1}^{i=90}S_{\max_i}}{90}=\frac{11558\text{ ft}}{90}\approx 128.4\text{ ft} \tag{4a,b}$$

$$\text{(a)} \quad q = \sum_{i=1}^{i=90} \frac{q_i}{n} = \frac{26.83}{90} = 0.298 \approx 0.3, \quad \text{(b)} \quad c = \sum_{i=1}^{i=90} \frac{c_i}{n} = \frac{130.38}{90} = 1.448 \approx 1.45 \quad \text{(5a,b)}$$

Above calculations show that speeds $V_{\max}^{sm}$ and $V_{\max}^{avg}$ (average) calculated by two different ways-formulas (3a,b) almost coincide each other. The same thing takes place with the coordinates $S_{\max}^{sm}$ and $S_{\max}^{avg}$ (average) also calculated by two different ways-formula (4a,b).

<u>The results of calculations based on the data of the Table 2</u>

$$\text{(a)} \quad V_0^{sm} = \frac{\sum_{i=1}^{i=90} V_{0_i} \cdot S_{0_i}}{\sum_{i=1}^{i=90} S_{0_i}} = \frac{585070 \text{ MPH} \cdot \text{ft}}{22633 \text{ ft}} \approx 25.85 \text{ MPH},$$

$$\text{(b)} \quad V_0^{sm} = \frac{\sum_{i=1}^{i=90} V_{0_i}}{90} = \frac{2327 \text{ MPH}}{90} \approx 25.86 \text{ MPH} \quad \text{(6a,b)}$$

$$\text{(a)} \quad S_0^{sm} = \frac{\sum_{i=1}^{i=90} V_{0_i} \cdot S_{0_i}}{\sum_{i=1}^{i=90} V_{0_i}} = \frac{585070 \text{ MPH} \cdot \text{ft}}{2327 \text{ MPH}} \approx 251.43 \text{ ft},$$

$$\text{(b)} \quad S_0^{avg} = \frac{\sum_{i=1}^{i=90} S_{0_i}}{90} = \frac{22633 \text{ ft}}{90} \approx 251.48 \text{ ft} \quad \text{(7a,b)}$$

$$\text{(a)} \quad v = \sum_{i=1}^{i=90} \frac{v_i}{n} = \frac{52.62}{90} = 0.585 \approx 0.59, \text{ (b)} \quad h = \sum_{i=1}^{i=90} \frac{h_i}{n} = \frac{93.28}{90} = 1.04 \text{ (8a,b)}$$

Here also calculations show that speeds V_0^{sm} and V_0^{avg} (average) calculated by two different ways-formulas (6a,b) almost coincide each other. The same thing takes place with the coordinates S_0^{sm} and S_0^{avg} (average) also calculated by two different formulas (7a,b). For further calculations we simplified all of our notations, and now they are denoted as: $V_{\max}^{sm} \approx V_{\max}^{avg} = V_{\max}$, $S_{\max}^{sm} \approx S_{\max}^{avg} = S_{\max}$ and $S_0^{sm} \approx S_0^{avg} = S_0$.

<u>The results of calculations based on the data of the Table 3</u>

$$V_{\min} = 0, \quad S_{\min}^{avr} = \frac{\sum_{i=1}^{i=90} S_{\min_i}}{90} = \frac{31389 \text{ ft}}{90} \approx 348.7 \text{ ft}, \quad r = \sum_{i=1}^{i=90} \frac{r_i}{n} = \frac{73.02}{90} = 0.81 \quad (9)$$

Obviously, that having the value of the entering speed $V_0 = 25 \text{ MPH}$, the value of the length of the additional lane $L = 430 \text{ ft}$ and the values of the coefficients $c = 1.45$, $q = 0.30$, $h = 1.04$, $v = 0.59$ and as shown in **Table 4**, then based on 5 × 5 determinants, developed in [41], the constant coefficients *A*, *B*, *C*, *D*, and *E*, of Equation (1) can be found. However, here there is an alternative way to find those coefficients. For that porpoise here it is considered the initial

Table 4. A list of coefficients.

Coefficients	*c*	*q*	*h*	*v*	*r*
Their values	1.45	0.30	1.04	0.59	0.81

conditions, related to the crucial points of the curve $V(S)$, such as $(0;25\text{ MPH})$, $(S_{\max};V_{\max})$, $(S_0;25\text{ MPH})$, $(S_{\min};0)$, $[S_{\max};a(S_{\max})=0]$ and $[S_{\min};a(S_{\min})=0]$. On the base that the system of linear equations with five unknowns and five equations is obtained. Below is the system of those equations:

$$\begin{aligned}
&A\cdot S_{\max}^4+B\cdot S_{\max}^3+C\cdot S_{\max}^2+D\cdot S_{\max}+E=\frac{11.2}{S_{\max}^2}\\
&A\cdot S_{\min}^4+B\cdot S_{\min}^3+C\cdot S_{\min}^2+D\cdot S_{\min}+E=-\frac{25}{S_{\min}^2}\\
&A\cdot S_0^4+B\cdot S_0^3+C\cdot S_0^2+D\cdot S_0+E=0\\
&A\cdot 6S_{\max}^4+B\cdot 5S_{\max}^3+C\cdot 4S_{\max}^2+D\cdot 3S_{\max}+E\cdot 2=0\\
&A\cdot 6S_{\min}^4+B\cdot 5S_{\min}^3+C\cdot 4S_{\min}^2+D\cdot 3S_{\min}+E\cdot 2=0
\end{aligned}\tag{10}$$

Solution of this system of equations with $S_{\max}^{avr}=S_{\max}^{sm}=S_{\max}=0.024375\text{ Mi}$, $S_{\min}^{avr}=S_{\min}^{sm}=S_{\min}=0.066042\text{ Mi}$ and $S_0^{avr}=S_0^{sm}=S_0=0.047621\text{ Mi}$ allowed to find those coefficients with very high accuracy. Using online "5 × 5 Matrix Determinant Calculator" allowed to calculate those coefficients very precise and very quick. Calculated values of these coefficients are:

$$A=19572057512.000000\,\frac{\text{MPH}}{\text{Mi}^6},\quad B=-3650562365.000000\,\frac{\text{MPH}}{\text{Mi}^5},$$

$$C=258753734.623000\,\frac{\text{MPH}}{\text{Mi}^4},\quad D=-8787907.385580\,\frac{\text{MPH}}{\text{Mi}^3}\ \text{and}$$

$$E=125278.962402\,\frac{\text{MPH}}{\text{Mi}^2}.$$

As it can be seen, in this considered case the leading coefficient *A*is positive (*A*>0). It has to be noted that because the speed of vehicles is given in MPH, so in further calculations all of considered distances (*L*, $S_{\max}$, $S_{\min}$ and S_0) given in feet have been converted to miles. Thus, calculation all of coefficients will allow to find the final form of equations for velocity $V(S)$ as well as for acceleration/deceleration $a(S)$. As shown below in **Figure 1** and **Figure 2**, the view of the graphs $V(S)$ and $a(S)$, belongs to this considered version, when leading coefficient $A>0$.

As we show above one of the major component of the delay is the time spending of a vehicle from the entry of the additional lane ($S=0$) up to the end of queue ($S=S_{\min}=0.066042\text{ Mi}$). Obviously, that that time could be found as division of the covered distance $S_{\min}=0.066042\text{ Mi}$ over the average speed of the vehicle, that is: $T_0=\frac{S_{\min}}{V(s)_{avg.}}$. Average speed will be found as $V(s)_{avg.}=\frac{\int_0^{S_{\min}}V(s)\mathrm{d}s}{S_{\min}}$. So, after integration and division and then inserting the consequent values of the coefficients A,B,C,D,E and distance $S_{\min}$ into the equation for $V(s)_{avg.}$ the average speed will be found as:

$$\begin{aligned}V(s)_{avg}&=\frac{A}{7}\cdot S_{\min}^6+\frac{B}{6}\cdot S_{\min}^5+\frac{C}{5}\cdot S_{\min}^4+\frac{D}{4}\cdot S_{\min}^3+\frac{E}{3}\cdot S_{\min}^2+25\text{ MPH}\\&\approx 25.808\text{ MPH}\end{aligned}\tag{11}$$

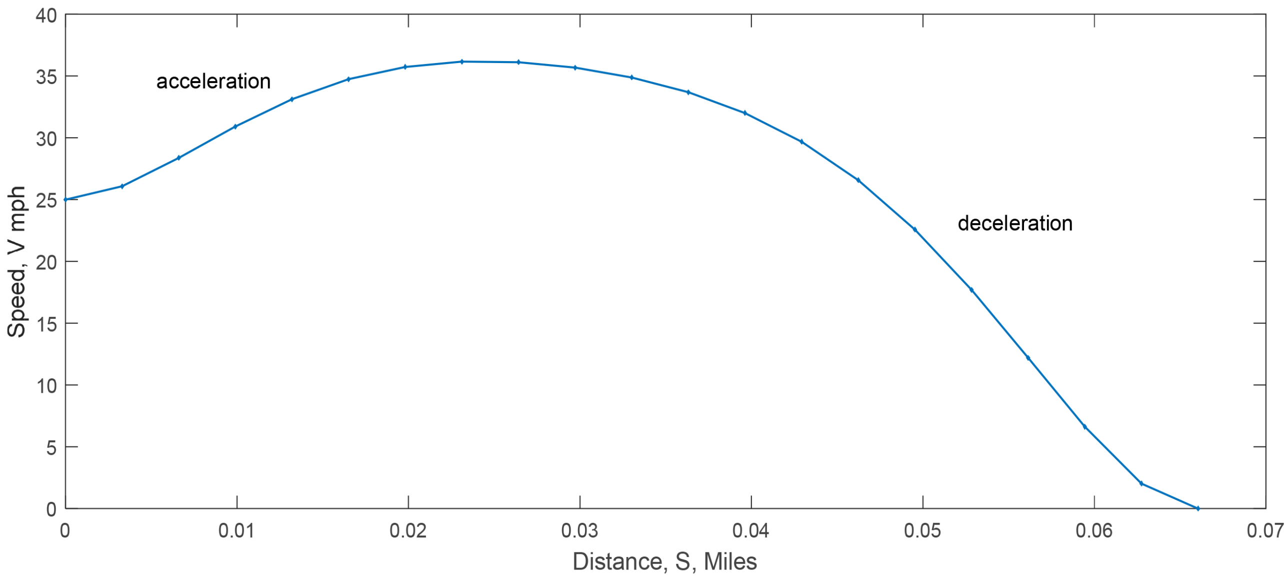

Figure 1. Velocity V as a Function of Distance S when A > 0.

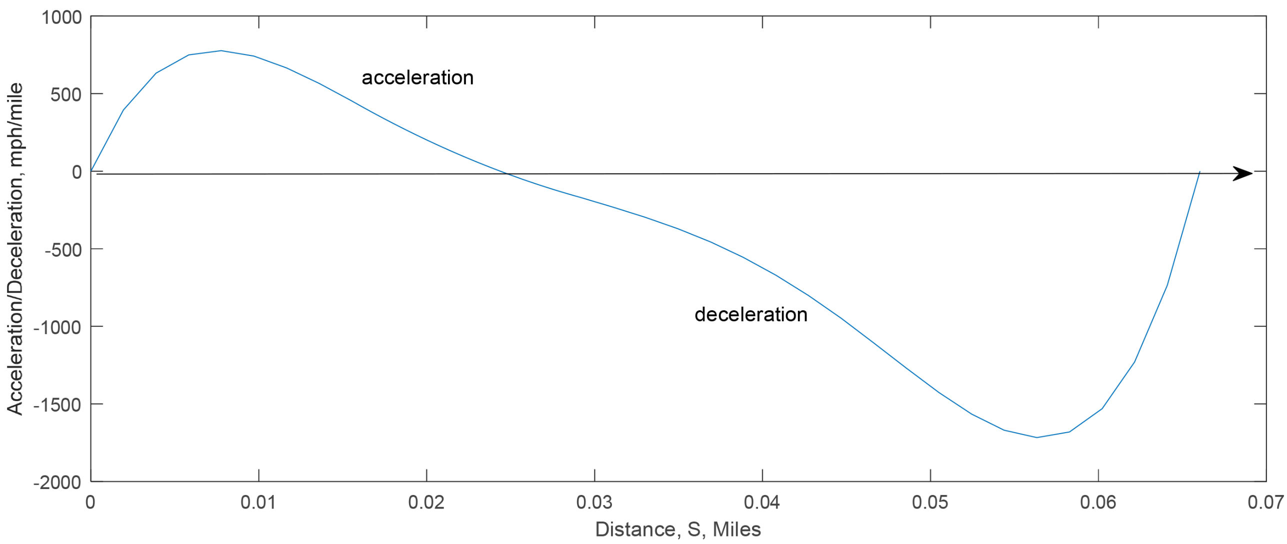

Figure 2. Acceleration/Deceleration a(S) as a Function of Distance S when A > 0.

Hence, the consequent delay time will be:

$$T_d = \frac{S_{\min}}{V(s)_{avg.}} = \frac{0.066042 \text{ Mi}}{25.808 \text{ MPH}} = 9.2123 \text{ sec} \approx 9.21 \text{ sec} \tag{12}$$

Thus, all of above calculations, based on data of hypothetic statistic model, which is related to the simulation of the kinematics of the vehicles, show the perfect rightfulness of our proposed method regarding to representation the movements of the vehicles in the additional lane of roundabouts as the 6th order polynomial function. Because $S_{\min(1)} = 0$, $S_{\min(2)} = S_{\min} \approx 348.7 \text{ ft}$, $S_{\max} \approx 128.7 \text{ ft}$, so according to the above diagram, illustrated on **Figure 1** the braking distant can be estimated as: $L_{br} = S_{\min} - S_{\max} \approx 220 \text{ ft}$. Previously, using the data of **Tables 1-3** and formulas (4a,b) and (9) the hypothetical-statistical medium values and the average values of the distances $S_{\max}^{sm}$, $S_{\max}^{avg}$ and $S_{\min}$ have been calculated. At the same time using the condition for the first derivatives of the analytic function (1), represented the velocity $V(s)$, there were founded almost the same values of those distances. The calculation shows that the first derivative of this function have zero values when $S_1 = 0$, $S_2 = 128.3\text{ ft}$ and $S_3 = 348.5\text{ ft}$. Thus, the calculated distance between S_3 and S_2 also represents the braking distance, and it will be $L_{avg}^{br} = 348.5 - 128.3 \approx 220.2\text{ ft}$. Hence, there is very good agreement between the values L_{avg}^{br} and L_{br} calculated on the base of the analytic formula (1) and the hypothetical-statistical method of data collections consequently. Therefore, in this considered case the length of the queue can be calculated as the different of two distances, that is:

$$L_{que.} = L - S_{\min} \approx 430\text{ ft} - 348.5\text{ ft} = 81.5\text{ ft}. \quad (13)$$

Now, as an example, from the above considered 90 vehicles we have chosen the first 6 initial simulation runs, where vehicles queued one after one. For these vehicles it will be estimated individual delay of each one and then calculate their average delay. Here some hypothetical-statistical data were collected for 5 vehicles (included the passenger cars, a motorcycle, a light-duty truck and a mini or limo-bus) already queued before "Yield" sign and the data for the 6th vehicle, just arriving to the end of queue. All of these vehicles waiting for to merge with the roundabout traffic. It must be noted that transportation research indicated that the average length of the passenger vehicles lies from 15 ft to 16 ft (4.2 to 4.9 meters). The calculation of the average car length has said to be equal to the length of an Audi A4, that is 4500 mm, or we can say 14.7 ft. This is the length of a medium-sized car and obviously that not every car is like this. It is well known that the vehicles in the queue moving in the "stop-acceleration-deceleration-stop" regime. Therefore, the observation of traffic shows that average speed (with the consideration of the acceleration, deceleration and stopping regimes) of the vehicles in the queue approximately equal to 5 MPH. Estimation of the delay of each individual vehicle will allow to calculate the average delay of the given queueing. However, for that purpose, here it has to be noted that depend on the capacity of the vehicles (veh/hr) in the additional entry lane and as well as in the roundabout the hypothetical-statistical value of the time T_0, related to these conditions, may lie (approximate, with rounding up to second decimal) in the range $7 \le T_0 \le 9.21\text{ sec}$. Besides that, here it is assumed that completely queuing all of 6 incoming vehicles may take around 12 sec. Hence, based to these circumstances the consequent distance of the coordinate $S = S_{\min}$ from the end of additional lane $S = L$ may lie in the range from $70\text{ ft} \le d_0 \le 100\text{ ft}$. **Table 5** and **Table 6** represent the proper time parameters of those moving vehicles in the additional lane.

Average delay of the given queueing is calculated by the formula below

$$d_{av} = \frac{\sum_{i=1}^{i=6} d_{ad.ln_i}}{6} = \frac{=\sum_{i=1}^{i=6} (T_1 + T_2)_i}{6} \approx 70.59\text{ sec} \quad (14)$$

Table 5. Characteristics of moving vehicles.

Vehicles' number	1	2	3	4	5	6
Time T_0 (in sec)	9.07	7.32	8.23	9.08	7.54	9.21
Distance d_0 (in ft)	70	95	85	80	100	82
Stopping of the given vehicle behind of the:	"Yield" sign	Vehicle 1	Vehicle 2	Vehicle 3	Vehicle 4	Vehicle 5
Approximate time $T_{aprx(1)}$ (in sec) spending of the given vehicle for arriving and stopping behind of the noted place	11.42	10.51	7.65	5.73	4.84	0
The sum of these two times: $T_1 = T_0 + T_{aprx(1)}$	20.49	17.83	15.88	14.81	12.38	9.21

Table 6. Characteristics of vehicles in the queues.

Vehicles' number in queue	1	2	3	4	5	6
Approximate time $T_{aprx(2)}$ (in sec) spending of the given vehicle in the queue completely to approach to the "Yield" sign	0	2.12	5.25	7.17	9.34	11.51
Average stopping time $T_{av.stp}$ (in sec.) of the given vehicle before "Yield" sign	15.23	28.41	42.33	57.22	71.24	83.11
The sum of these two time periods $T_2 = T_{av.stp} + T_{aprx(2)}$	15.23	30.53	47.58	64.39	80.58	94.62
The delay $d_{ad.ln}$ (in sec) of each vehicle due to the additional second lane of the roundabout can be found as $d_{ad.ln} = T_1 + T_2$	35.72	48.36	63.46	79.20	92.96	103.83
Average delay d_{av} (in sec) of these 6 vehicles or queue	70.59					

Obviously that T_1 in **Table 5** is the time spending i^{th} driver to move a vehicle through the additional lane of the roundabout, started from the point $S_{\min(1)} = 0$ up to its totally stopping behind consequent n^{th} ($n = 1,2,3,4,5$) vehicle or behind the "Yield" sign. In the **Table 6** T_2 is the time spending the same driver to move a vehicle in the queue, beginning from the stopping points up to the position when driver has to wait for merging with the roundabout traffic. Therefore, the delay due to just additional lane of the roundabout will be the sum of these two intervals of time. However, it is obviously that this fraction of the total delay will be equal to the delay of the 6th vehicle of the queue, that is $d_{ad.ln} = 103.83$ sec (**Table 6**). Just it should be pointed out that calculation module of the existing delay in one entering lane is based on procedures in the Highway Capacity Manual. This method of estimation of the entering and queuing delays due to the additional entry lane will help roundabout designer to have preliminary judgment about choosing of the length of that line and it will help to save money and time in designing.

Now, in order to find the total delay, it must be considered also the delay due to within area of the given roundabout. Here it have be noted that now for safety purpose the speed limit in roundabouts ranges from 15 ÷ 20 mph. Obviously, that the driving time in roundabout will also depend on the capacity of roundabout (veh/hr), its size (small, medium or large) and the medium permissible speed of the vehicles. The diameter of the small, single lane roundabout lies in the range from 110 ft to 150 ft, the diameter of the medium, two lane roundabout lies in the range from 150 ft to 230 ft and the diameter of the large, three lane roundabout lies in the range from 200 ft to 260 ft. Let's assume that the observed medium speeds of the vehicles on those roundabouts are15 MPH for small, 17 MPH for medium and 20 MPH for large roundabouts. However, in each particularly considered case entering in the roundabout vehicle will accelerate from the speed $V(s)=0$ and decelerate close to the consequent exit zone of the roundabout. For further calculations we consider that the average diameter of the small roundabout is (110 + 150) ft/2 = 130 ft, the medium roundabout is (150 + 230) ft/2 = 190 ft and the large roundabout is (200 + 260) ft/2 = 230 ft. Most widespread and most common roundabouts have four single or multi lane entrances and the same amounts of the exits. Therefore, our considered 6 vehicles may occupy the second, the third, the fourth exits or just one of them. Based on these circumstances, the estimated time when merged in the roundabout vehicles will completely leave those three available exits of the given roundabout are shown in **Table 7**.

The total delay of 6 vehicles or their total enter-exit time (related to the given roundabout) can be represented as the sum of the delay $d_{ad.ln}$ and delays $d_{s.r.}$, $d_{m.r.}$ and $d_{l.r.}$ accordingly, that is $d_{sm}=d_{ad.ln}+d_{s.r.}$, $d_{md}=d_{ad.ln}+d_{m.r.}$ and $d_{lg}=d_{ad.ln}+d_{l.r.}$. **Tables 8-10** representing the total delays of the vehicles and these tables are obtained on the base of **Table 6** and **Table 7**.

Now we will consider the case when all of 6 vehicles have left the same exit zone of the given roundabout. Obviously, that in this case the time required for totally leaving all of those vehicles the given exit zone of a roundabout will be equal the sum of two delays: the delay $d_{ad.ln}$ of the 6th vehicle due to the additional second lane of the given roundabout (**Table 6**) and the delay $d_{l.r.}$ or time $T_{l.r.}$ spending of that vehicle for completely entering the given exit zone of the same roundabout (**Table 7**). **Table 11** below represents that time.

Missing all intermediate calculations and tables we have developed similar to **Table 6** the additional **Table 12** represented most of above considered 90 vehicles. Because in **Table 6** already considered the first 6 vehicles, therefore in developed **Table 12** it is considered remaining 84 vehicles. Here we have taken into consideration 14 simulated runs where each of them contains 6 different types of vehicles, such as (like above) passenger cars, light-duty trucks, mini or limo-buses

Table 7. Vehicle travel times at roundabouts.

Leaving the exits zones of the roundabouts	First	Second	Third
Delay $d_{s.r.}$ (in sec) or time $T_{s.r.}$ (in sec) spending a vehicle for completely entering the given exit of the *small* roundabout.	4.34	9.29	13.51
Delay $d_{m.r.}$ (in sec) or time $T_{m.r.}$ (in sec) spending a vehicle for completely entering the given exit of the *medium* roundabout.	5.46	11.22	17.27
Delay $d_{l.r.}$ (in sec) or time $T_{l.r.}$ (in sec) spending a vehicle for completely entering the given exit of the *large* roundabout.	6.42	12.15	18.06

Table 8. Total delay of vehicles at small roundabouts.

Leaving the exits zones of the *small* roundabout	First	Second	Third
Total delay d_{sm} (in sec) of the vehicle N1completely left given exit:	40.06	45.01	49.23
Total delay d_{sm} (in sec) of the vehicle N2completely left given exit:	52.70	57.65	61.87
Total delay d_{sm} (in sec) of the vehicle N3completely left given exit:	67.80	72.75	76.97
Total delay d_{sm} (in sec) of the vehicle N4completely left the given exit:	83.54	88.29	92.71
Total delay d_{sm} (in sec) of the vehicle N5completely left the given exit:	97.30	102.25	106.47
Total delay d_{sm} (in sec) of the vehicle N6completely left the given exit:	108.17	113.12	117.34

Table 9. Total delay of vehicles at medium roundabouts.

Leaving the exits zones of the *medium* roundabout	First	Second	Third
Total delay d_{md} (in sec) of the vehicle N1completely left given exit:	41.18	46.94	52.99
Total delay d_{md} (in sec) of the vehicle N2completely left given exit:	53.82	59.58	65.63
Total delay d_{md} (in sec) of the vehicle N3completely left given exit:	68.92	74.68	80.73
Total delay d_{md} (in sec) of the vehicle N4completely left given exit:	84.66	90.42	96.47
Total delay d_{md} (in sec) of the vehicle N5completely left given exit:	98.42	104.18	110.23
Total delay d_{md} (in sec) of the vehicle N6completely left given exit:	109.29	115.05	121.10

Table 10. Total delay of vehicles at large roundabouts.

Leaving the exits zones of the *large* roundabout	First	Second	Third
Total delay d_{lg} (in sec) of the vehicle N1completely left given exit:	42.14	47.87	53.78
Total delay d_{lg} (in sec) of the vehicle N2completely left given exit:	54.78	60.51	66.42
Total delay d_{lg} (in sec) of the vehicle N3completely left given exit:	69.88	75.61	81.52
Total delay d_{lg} (in sec) of the vehicle N4completely left given exit:	85.62	91.35	97.26
Total delay d_{lg} (in sec) of the vehicle N5completely left given exit:	99.38	105.11	111.02
Total delay d_{lg} (in sec) of the vehicle N6completely left given exit:	110.25	115.98	121.89

Table 11. A summary of total vehicle delays.

All of vehicles leaving *the same exit zone* of the *small* roundabout	**First**	**Second**	**Third**
Total delay all of vehicles completely leaving the given exit zone:	108.17	113.12	117.34
All of vehicles leaving *the same exit zone* of the *medium* roundabout	**First**	**Second**	**Third**
Total delay all of vehicles completely leaving the given exit zone:	109.29	115.05	121.10
All of vehicles leaving *the same exit zone* of the *large* roundabout	First	Second	Third
Total delay all of vehicles completely leaving the given exit zone:	**110.25**	**115.98**	**121.89**

and motorcycles. Each of these 14 simulated runs may have its own combination of these noted vehicles. These 14 simulated runs, represented in this model (possessing stochastic nature), were initially executed using random number seeds,

Table 12. Vehicle delays based on simulation runs.

Simulation runs by the order of the vehicles	**1 (7 ÷ 12)**						**2 (13 ÷ 18)**					
Number of vehicles	**7**	**8**	**9**	**10**	**11**	**12**	**13**	**14**	**15**	**16**	**17**	**18**
Delay $d_{ad.ln}$ (in sec)	31.19	50.58	59.94	82.44	87.51	98.82	28.63	49.71	60.54	80.23	89.31	96.45
Average delay d_{av} (in sec)	68.41						67.47					
Simulation runs by the order of the vehicles	**3 (19 ÷ 24)**						**4 (25 ÷ 30)**					
Number of vehicles	**19**	**20**	**21**	**22**	**23**	**24**	**25**	**26**	**27**	**28**	**29**	**30**
Delay $d_{ad.ln}$ (in sec)	29.67	42.45	58.76	77.34	92.32	99.12	33.64	48.54	61.86	85.36	90.27	97.56
Average delay d_{av} (in sec)	66.61						69.54					
Simulation runs by the order of the vehicles	**5 (31 ÷ 36)**						**6 (37 ÷ 42)**					
Number of vehicles	**31**	**32**	**33**	**34**	**35**	**36**	**37**	**38**	**39**	**40**	**41**	**42**
Delay $d_{ad.ln}$ (in sec)	32.12	45.56	63.97	74.85	94.61	101.14	34.78	51.55	56.29	88.78	94.43	100.31
Average delay d_{av} (in sec)	68.71						71.04					
Simulation runs by the order of the vehicles	**7 (43 ÷ 48)**						**8 (49 ÷ 54)**					
Number of vehicles	**43**	**44**	**45**	**46**	**47**	**48**	**49**	**50**	**51**	**52**	**53**	**54**
Delay $d_{ad.ln}$ (in sec)	34.62	51.78	56.33	79.84	88.17	99.87	27.74	48.35	65.75	75.21	95.18	103.63
Average delay d_{av} (in sec)	68.44						69.31					
Simulation runs by the order of the vehicles	**9 (55 ÷ 60)**						**10 (61 ÷ 66)**					
Number of vehicles	**55**	**56**	**57**	**58**	**59**	**60**	**61**	**62**	**63**	**64**	**65**	**66**
Delay $d_{ad.ln}$ (in sec)	28.75	44.56	63.21	83.42	92.14	100.31	35.98	48.36	61.76	77.52	90.22	98.43
Average delay d_{av} (in sec)	68.73						68.71					
Simulation runs by the order of the vehicles	**11 (67 ÷ 72)**						**12 (73 ÷ 78)**					
Number of vehicles	**67**	**68**	**69**	**70**	**71**	**72**	**73**	**74**	**75**	**76**	**77**	**78**
Delay $d_{ad.ln}$ (in sec)	31.86	49.51	59.64	80.37	89.57	96.14	34.15	43.75	57.39	84.62	93.18	99.46
Average delay d_{av} (in sec)	67.85						68.76					
Simulation runs by the order of the vehicles	**13 (79 ÷ 84)**						**14 (85 ÷ 90)**					
Number of vehicles	**79**	**80**	**81**	**82**	**83**	**84**	**85**	**86**	**87**	**88**	**89**	**90**
Delay $d_{ad.ln}$ (in sec)	32.43	50.86	60.38	81.91	89.16	99.19	29.46	49.73	58.39	76.40	93.59	101.17
Average delay d_{av} (in sec)	69.00						68.12					

with their arbitrary values, close to the existing actual seed values. Based on this model the created Table 12 introduces the hypothetical-statistical representation of the average results of these 14 simulated runs. It can be noted that since VISSIM

Table 13. Average vehicle delays with the additional entry lane.

Simulation runs	1	2	3	4	5	6	7
Average delays $d_{av}^{a.l.}$ (in sec) due to the entry of the roundabout with the additional entry lane	70.59	68.41	67.47	66.61	69.54	68.71	71.04
Average delays $d_{av}^{s.l.}$ (in sec) due to the entry of the roundabout with the single-entry lane	104.52	109.71	103.28	100.16	110.43	106.18	105.35
The gain coefficient of the delays $K = \frac{d_{av}^{a.l.}}{d_{av}^{s.l.}}$	0.68	0.62	0.65	0.67	0.63	0.65	0.67
The gain in terms of the percentage %	32	38	35	33	37	35	33
Average of the coefficients K				0.64			
Average of the delays $d_{av}^{a.l.}$ (in sec)				68.75			
Average of delays $d_{av}^{s.l.}$ (in sec)				107.97			
The gain coefficient based on these averages				0.64			
Average gain in percentage %				36.13			

is a stochastic model whose results vary depending on the random seed number used, the model usually running multiple times and the average results are used. In the Table 12 the average delay is calculated by formula (14) and this Table also have been generated on the base of the hypothetical-statistical method, Now, using the hypothetical-statistical method we have considered the coefficient K represented the gain of the delay when an additional entry lane of roundabout is added. For that purpose, Table 13 is created, contained average delays of the above considered 15-simulation runs. Besides that, the tables represented interpolated average delays of the same amount (15) of the simulation runs, but related to the actual, single-entry lane roundabout, also observed at the same rush hour time.

So, the average delay of each run $d_{av.r}$ will be the average of the sum of the average delays $d_{av.i}$ all 15-simulation runs, that is

$$d_{av.r} = \frac{\sum_{i=1}^{i=15} d_{av.i}}{15} = \frac{1031.29 \text{ sec}}{15} = 68.75 \text{ sec}.$$

In our research have been considered also the case, when the leading coefficient A of the general equation of movement (1) is negative ($A < 0$). Missing all intermediate calculations and similar to the above created tables (serving as the base for those calculations) here it is present the values of the constant coefficients A, B, C, D, and E of the general Equation (1), estimated for this particular case.

$$A = -7641961565.5700000 \frac{\text{MPH}}{\text{Mi}^6}, \quad B = 1282149367.4000000 \frac{\text{MPH}}{\text{Mi}^5},$$

$$C = -52880859.5282000 \frac{\text{MPH}}{\text{Mi}^4}, \quad D = -802223.5216970 \frac{\text{MPH}}{\text{Mi}^3} \text{ and}$$

$$E = 53952.6883597 \frac{\text{MPH}}{\text{Mi}^2}.$$

Here the average values of the significant distances are: $S_{\max}^{avr} = 0.0244318$ Mi, $S_0^{avr} = 0.0397017$ Mi and $S_{\min}^{avr} = 0.0651515$ Mi. As shown below in **Figure 3** and **Figure 4**, the view of the graphs $V(s)$ and $a(s)$, belongs to this considered version when the leading coefficient $A < 0$.

On the base of simulation of the delay data on **Figure 5** it is represented hypothetical-statistical graphical model showing the relationship between the gain g (%) of delay (in percentage) and the additional lane length L (ft).This Model have been approximated very well and represented as the analytic exponential function with the form $g = 78.1\mathrm{e}^{-0.001737L}$, where changing of the L in the range $150\text{ ft} \le L \le 550\text{ ft}$ leads to the changing of g in the range $60\% > g > 30\%$.

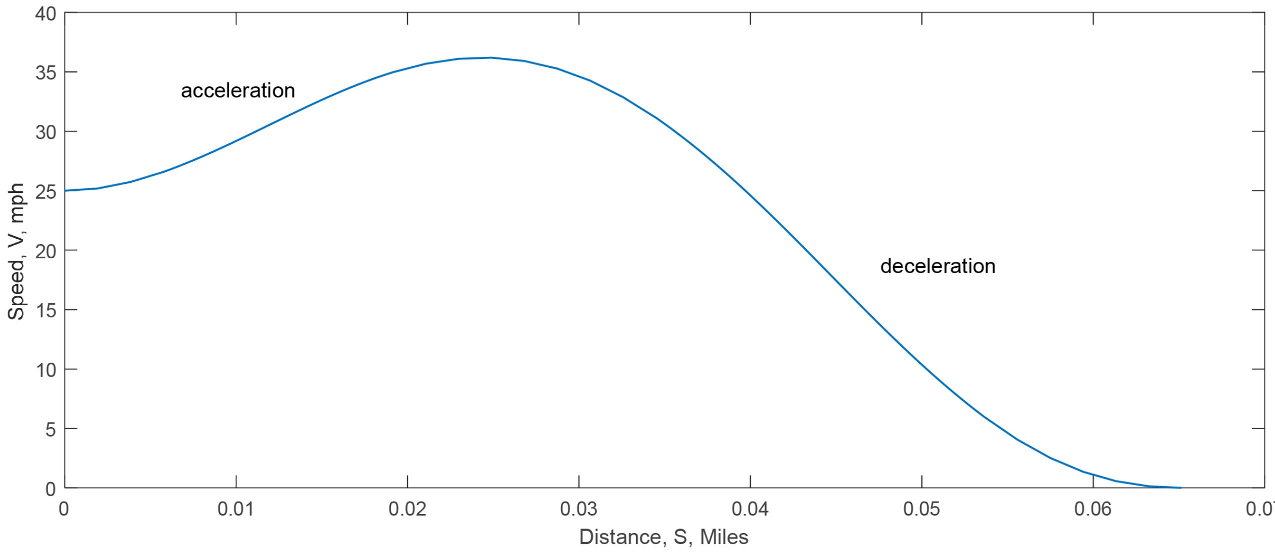

Figure 3. Velocity V as a Function of Distance S when A < 0.

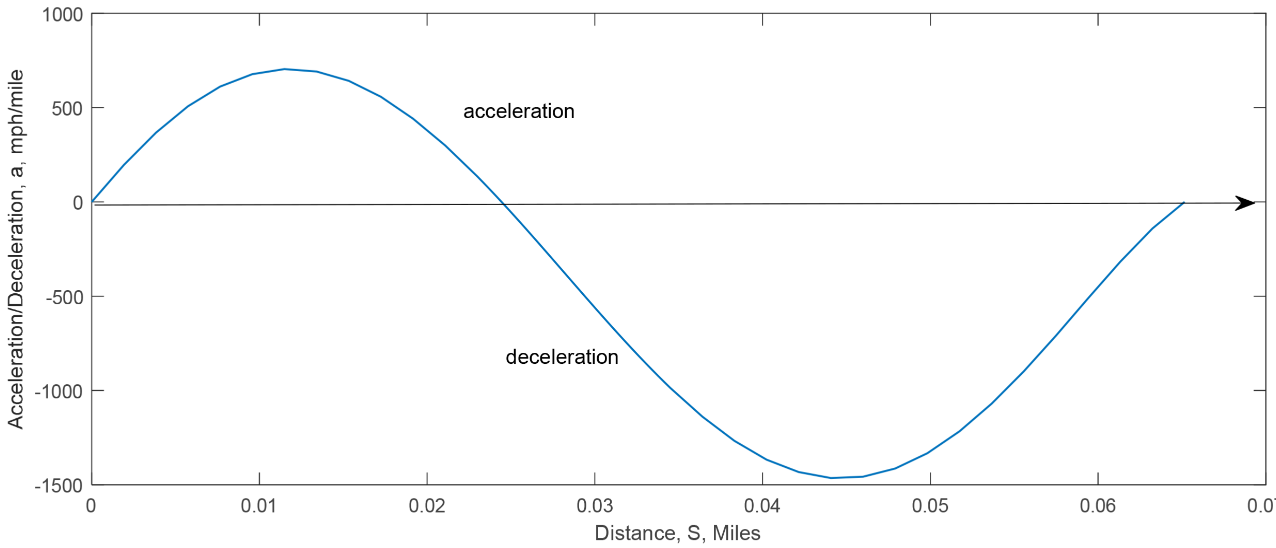

Figure 4. Acceleration/Deceleration a(S) as a Function of S when A < 0.

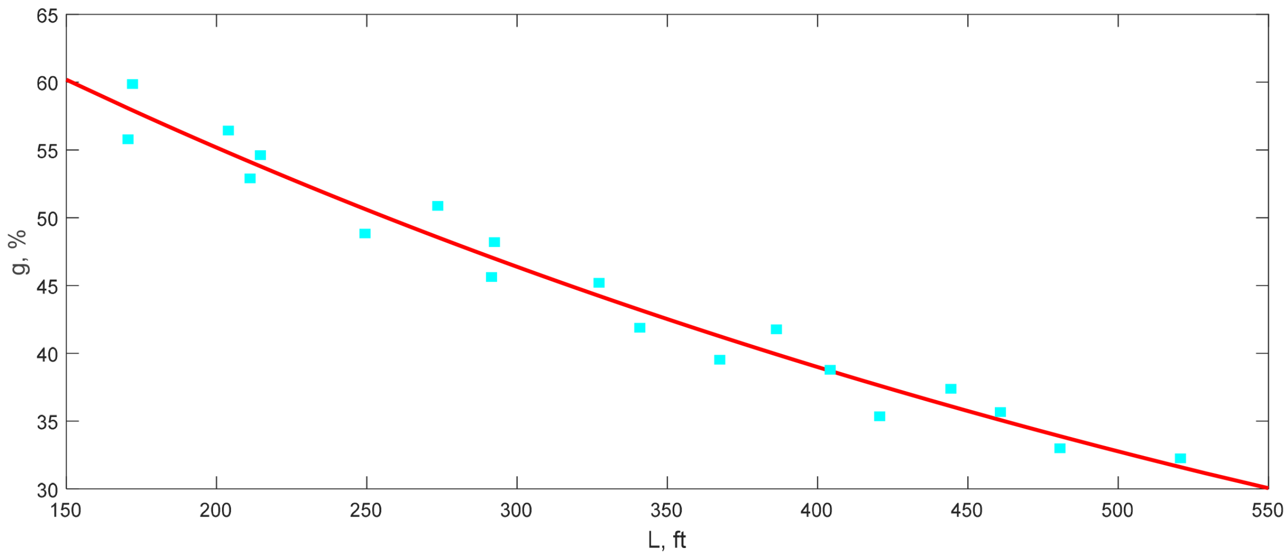

Figure 5. The Delay's Gain g (%) versus Additional Lane Length L (ft).

Now it is very important to realize the reason why in these considered two case the leading coefficient A of Equation (1) may have as positive ($A>0$) as well as negative ($A<0$) signs. For that purpose, the kinematics of movement of two consequent vehicles, represented these two cases, were investigated. Then it has been done comparative analysis of such parameters of those two movements as their average velocities, their average accelerations/decelerations, and their partial and total delays. Calculation of these parameters are performed in the following intervals of changing of S: $0 \le S \le S_{\max}$, $S_{\max} \le S \le S_{\min}$ and $0 \le S \le S_{\min}$. Because the constant coefficients A, B, C, D, and E already are known, so based on the formulas (1) and (2) the above mentioned parameters were calculated. These parameters have been calculated in respect to the time as well as in respect to the distance. Below are the values of the seeking parameters, calculated for the case $A>0$ and for the consequent ranges of changing of S:

1) In the range of changing of S, $0 \le S \le S_{\max}$: $V(s)_{avg(1,1)} = 31.6135\ \text{MPH}$, $a(s)_{avg(1,1)} = 459.4865 \dfrac{\text{MPH}}{\text{Mi}}$. Based on the formula (12) the value of the partial delay is calculated: $t_{d(1,1)} = 2.7757\ \text{sec}$. Because $V(0) = 25\ \text{MPH}$, $V(s_{\max}) = V_{\max} = 36.2\ \text{MPH}$ and $t_{d(1,1)} = 2.7757\ \text{sec}$, so here the calculated value of acceleration is: $a(t)_{avg(1,1)} = 4.035 \dfrac{\text{MPH}}{\text{sec}}$. Therefore, in this interval of time $t_{d(1,1)}$ the speed of the vehicles can be expressed as:

$$V(t)_{(1,1)} = V_0 + a(t)_{avg(1,1)} \cdot t = 25 + 4.035 \cdot t \tag{15}$$

2) In the range of changing of S, $S_{\max} \le S \le S_{\min}$: $V(s)_{avg(1,2)} = 23.3043\ \text{MPH}$, $a(s)_{avg(1,2)} = -868.7917 \dfrac{\text{MPH}}{\text{Mi}}$. The calculated value of the partial delay, regard-

ing to this range of changing of *S* is: $t_{d(1,2)} = 6.4366\ \text{sec}$. Because $V(s_{\max}) = 36.2\ \text{MPH}$, $V(s_{\min}) = 0$ and $t_{d(1,2)} = 6.4366\ \text{sec}$, so here the average value of the calculated deceleration will have the value $a(t)_{avg(1,2)} = -5.6241\frac{\text{MPH}}{\text{sec}}$. Hence, in this interval of time $t_{d(1,2)}$ the speed of the vehicles will have the form:

$$V(t)_{(1,2)} = V_{\max} + a(t)_{avg(1,2)} \cdot t = 36.2 - 5.6241 \cdot t \tag{16}$$

3) In the range of changing of *S*, $0 \le S \le S_{\min}$: $V(s)_{avg(1,3)} = 25.808\ \text{MPH}$, $a(s)_{avg(1,3)} = -378.5464\frac{\text{MPH}}{\text{Mi}}$. The calculated value of the total delay, regarding to this range of changing of *S* is:
$t_{d(1,3)} = T_{d_1} = 2.7757\ \text{sec} + 6.4366\ \text{sec} = 9.2123\ \text{sec}$. Here the average value of acceleration/deceleration in terms of time is estimated as:

$$a(t)_{avg(1,3)} = \frac{a(t)_{avg(1,1)} \cdot t_{d(1,1)} + a(t)_{avg(1,2)} \cdot t_{d(1,2)}}{t_{d(1,3)}} = -2.7138\frac{\text{MPH}}{\text{sec}} \tag{17}$$

Hence, in result of this in this interval of time $t_{d(1,3)}$ the velocity can be represented (just formally) as:

$$V(t)_{(1,3)} = V_0 + a(t)_{avg(1,3)} \cdot t = 25 - 2.7138 \cdot t \tag{18}$$

<u>The ratios between consequent parameters.</u>

1) Speed $V(s)_{avg(1,1)}$ to speed $V(s)_{avg(1,2)}$: $R_1 = 1.3566$
2) Acceleration $a(t)_{avg(1,1)}$ to deceleration $a(t)_{avg(1,2)}$: $R_2 = -0.71745$
3) Acceleration $a(s)_{avg(1,1)}$ to deceleration $a(s)_{avg(1,2)}$: $R_3 = -0.52888$
4) Delay $t_{d(1,1)}$ to delay $t_{d(1,2)}$: $R_4 = 0.4312$

Below is shown the values of the seeking parameters, calculated for the case $A < 0$ and for the consequent ranges of changing of *S*:

5) In the range of changing of *S*, $0 \le S \le S_{\max}$: $V(s)_{avg(2,1)} = 30.67\ \text{MPH}$, $a(s)_{avg(2,1)} = 458.4191\frac{\text{MPH}}{\text{Mi}}$. Based on the formula (12) the value of the partial delay is calculated: $t_{d(2,1)} = 2.8678\ \text{sec}$. Because $V(0) = 25\ \text{MPH}$, $V(s_{\max}) = V_{\max} = 36.2\ \text{MPH}$ and $t_{d(2,1)} = 2.8678\ \text{sec}$, so here the calculated value of acceleration in terms of time is: $a(t)_{avg(2,1)} = 3.9054\frac{\text{MPH}}{\text{sec}}$.

So, in this interval of time $t_{d(2,1)}$ the speed of the vehicles in respect of time can be shown as:

$$V(t)_{(2,1)} = V_0 + a(t)_{avg(2,1)} \cdot t = 25 + 3.9054 \cdot t \tag{19}$$

6) In the range of changing of *S*, $S_{\max} \le S \le S_{\min}$:
$V(s)_{avg(2,2)} = 17.8708\ \text{MPH}$, $a(s)_{avg(2,2)} = -889.0049\frac{\text{MPH}}{\text{Mi}}$. The calculated value of the partial delay, regarding to this range of changing of *S* is:
$t_{d(2,2)} = 8.2028\ \text{sec}$. Because $V(s_{\max}) = 36.2\ \text{MPH}$, $V(s_{\min}) = 0$ and

$t_{d(2,2)} = 8.2028\ \text{sec}$, so here the value of deceleration in terms of time will be $a(t)_{avg(2,2)} = -4.4131\dfrac{\text{MPH}}{\text{sec}}$.

In this interval of time $t_{d(2,2)}$ the speed of the vehicles in terms of time will have the form:

$$V(t)_{(2,2)} = V_{\max} + a(t)_{avg(2,2)} \cdot t = 36.2 - 4.4131 \cdot t \quad (20)$$

6) In the range of changing of *S*, $0 \le S \le S_{\min}$ there are:

$V(s)_{avg(2,3)} = 22.6705\ \text{MPH}$, $a(s)_{avg(2,3)} = -383.7212\dfrac{\text{MPH}}{\text{Mi}}$. The calculated value of the total delay, regarding to this range of changing of *S* is:

$t_{d(2,3)} = t_{d(2,1)} + t_{d(2,2)} = T_{d_2} = 11.0706\ \text{sec}$. Here the average value of acceleration/deceleration in terms of time is estimated as:

$$a(t)_{avg(2,3)} = \frac{a(t)_{avg(2,1)} \cdot t_{d(2,1)} + a(t)_{avg(2,2)} \cdot t_{d(2,2)}}{t_{d(2,3)}} = -2.2582\frac{\text{MPH}}{\text{sec}}. \quad (21)$$

Hence, here also in the interval of time $t_{d(2,3)}$ the velocity can be represented (just formally) as:

$$V(t)_{(2,3)} = V_0 + a(t)_{avg(2,3)} \cdot t = 25 - 2.2582 \cdot t \quad (22)$$

The ratios between consequent parameters.

5) Speed $V(s)_{avg(2,1)}$ to speed $V(s)_{avg(2,2)}$: $R_5 = 1.7249$

6) Acceleration $a(t)_{avg(2,1)}$ to deceleration $a(t)_{avg(2,2)}$: $R_6 = -0.6920$

7) Acceleration $a(s)_{avg(2,1)}$ to deceleration $a(s)_{avg(2,2)}$: $R_7 = -0.51566$

8) Delay $t_{d(2,1)}$ to delay $t_{d(2,2)}$: $R_8 = 0.3496$.

As it can be seen from the comparison of the correspondent ratios $\dfrac{R_5}{R_1} = 1.272$, $\dfrac{R_6}{R_2} = 0.965$, $\dfrac{R_7}{R_3} = 0.975$ and $\dfrac{R_8}{R_4} = 0.8108$ here there are not big difference between the values R_2 and R_6 as well as R_3 and R_7. However, here it is indicated significant difference between the values R_1 and R_5 as well as R_4 and R_8 which is due to large difference between the velocities $V(s)_{avg(2,1)}$ and $V(s)_{avg(2,2)}$ ($\Delta V_1 \approx 12.8\ \text{MPH}$) and velocities $V(s)_{avg(1,1)}$ and $V(s)_{avg(1,2)}$ ($\Delta V_2 \approx 8.3\ \text{MPH}$). The ratio of these two differences of the velocities is substantial number, and it equal to $\delta = \dfrac{\Delta V_1}{\Delta V_2} \approx 1.5422$. Base on our investigation we can make a conclusion that in the formation of the sign of the leading coefficient *A* of Equation (1) the difference ΔV of the above noted velocities also may play certain role. Probably that low value of $\delta \approx 1$ implies positive sign of leading coefficient *A* and high value, negative. Therefore, because coefficient ausually may have as positive as well as negative signs, so in some cases it may have also zero value. Obviously, that in that cases the equation for velocity $V(s)$ will be represented by fifth degree polynomial functions. However, regardless from the sign of coefficient *A* and the degree of the polynomial function, sixth or five, in the region of investigation of vehicles' delays and kinematics (in the interval of changing S, $0 \le S \le S_{\min}$) the properties of that kinds of functions and characteristics of their graphs will remain unchangeable. That is, all of them will have minimums for $S = 0$ and $S = S_{\min}$, a maximum between them and the value of function $V(s_{\min}) = 0$ for $S = S_{\min}$. In addition, it has to be noted that above performed calculations also specified the following important circumstances: the first that durations of the acceleration times (partial delays) in both cases $A < 0$ and $A > 0$ almost the same: $t_{d(2,1)} - t_{d(1,1)} = 0.0921\ \text{sec}$. The second, that duration of the braking time (duration of deceleration or partial delay) in cases of $A < 0$ substantially higher than in case $A > 0$: $t_{d(2,2)} - t_{d(1,2)} \approx 1.77\ \text{sec}$. The third that based on the diagrams of velocities, represented in Figure 1 and Figure 3 here it can be done also the following conclusions: in both case ($A > 0$ and $A < 0$) these two graphs in different intervals of changing of S have different curvatures C_v. For our considered cases the general form of the formula used for calculation of the curvature has the following form.

$$C_v = \frac{\mathrm{d}^2 V(s)}{\mathrm{d}s^2} \cdot \left[1 + \left(\frac{\mathrm{d}V(s)}{\mathrm{d}s}\right)^2\right]^{-\frac{3}{2}} \tag{23}$$

Table 14 below represents the calculated values of this parameter.

Based on data of this Table the mean integrates values of curvature C_v for different intervals of changing of S are calculated. These calculations are done on the base of the following general formulas:

Table 14. Calculation of the curvatures based on leading coefficient.

Leading coefficient $A > 0$				Leading coefficient $A < 0$			
S_1	C_{v_1}	S_1	C_{v_1}	S_2	C_{v_2}	S_2	C_{v_2}
0.000000	250557.9248	0.0363231	-5.68×10^{-4}	0.000000	107905.3767	0.035833325	-5.898×10^{-5}
0.0033021	5.666×10^{-4}	0.0396252	-2.722×10^{-4}	0.003257575	2.651×10^{-3}	0.0390909	-2.377×10^{-5}
0.0066042	3.914×10^{-5}	0.0429273	-1.341×10^{-4}	0.00651515	3.319×10^{-3}	0.042348475	-8.010×10^{-6}
0.0099063	-8.1062×10^{-5}	0.0462294	-6.672×10^{-5}	0.009772725	6.98×10^{-5}	0.04560605	2.931×10^{-6}
0.0132084	$-2{,}701 \times 10^{-4}$	0.0495315	-3.315×10^{-5}	0.0130303	-3.672×10^{-5}	0.048863625	1.619×10^{-5}
0.0165105	-9.413×10^{-4}	0.0528336	-1.502×10^{-5}	0.016287875	-2.01×10^{-4}	0.0521212	4.279×10^{-5}
0.0198126	-5.605×10^{-3}	0.0561357	-1.87×10^{-6}	0.01954545	-9.872×10^{-4}	0.055378775	1.222×10^{-4}
0.0231147	-3.005×10^{-1}	0.0594378	2.01×10^{-5}	0.022803025	-2.569×10^{-2}	0.05863635	5.025×10^{-4}
0.0264168	-7.852×10^{-2}	0.0627399	1.721×10^{-4}	0.0260606	-2.432×10^{-2}	0.061893925	5.262×10^{-3}
0.0297189	-4.935×10^{-3}	0.066042	450,153.45	0.029318175	-8.533×10^{-4}	0.0651515	61,597.25
0.033021	-1.348×10^{-3}			0.03257575	-1.745×10^{-4}		

$$\text{a) } C_{v_{1,1}}^{mn.\text{int}} = \frac{\Delta S_1 \cdot \sum_{i=1}^{i=20} C_{v_{1i}}}{S_{\max_1}}, \text{ b) } C_{v_{1,2}}^{mn.\text{int}} = \frac{\Delta S_1 \cdot \sum_{i=1}^{i=20} C_{v_{1i}}}{S_{\min_1} - S_{\max_1}},$$

$$\text{c) } C_{v_{2,1}}^{mn.\text{int}} = \frac{\Delta S_2 \cdot \sum_{i=1}^{i=20} C_{v_{2i}}}{S_{\max_2}}, \text{ d) } C_{v_{2,2}}^{mn.\text{int}} = \frac{\Delta S_2 \cdot \sum_{i=1}^{i=20} C_{v_{2i}}}{S_{\min_2} - S_{\max_2}} \quad (24 \text{ a, b, c, d})$$

where $\Delta S_1 = \frac{S_{\min_1}}{20} = \frac{0.066042}{20} = 0.0033021$, $S_{\max_1} = 0.024375$,

$\Delta S_2 = \frac{S_{\min_2}}{20} = \frac{0.0651515}{20} = 0.003257575$, $S_{\max_2} = 0.0244318$.

As it can be seen from **Table 14**, if in the intervals $0 \le S \le S_{\min}$ to exclude the extreme values of the curvature (for $S = 0$ and for $S = S_{\min}$) and to consider just its minor values than the mean integrated (digitally, based on the tables data) values of the curvatures for the consequent intervals of changing of *S* will be: in the interval $0 < S \le S_{\max_1}$ for $A > 0$ the mean integrated value of curvature $C_{v_{1,1}}^{\text{mn.int}} = -4.156 \times 10^{-2}$ and for $A < 0$ it has value $C_{v_{2,1}}^{\text{mn.int}} = -2.783 \times 10^{-3}$. In the interval $S_{\max_1} \le S < S_{\min_1}$ ($A > 0$) the mean integrated value of curvature $C_{v_{1,2}}^{\text{mn.int}} = -6.778 \times 10^{-3}$ and in the interval $S_{\max_2} \le S < S_{\min_2}$ ($A < 0$) it has value $C_{v_{2,2}}^{\text{mn.int}} = -1.138 \times 10^{-3}$. The ratios between the consequent values of the curvatures are: 1) $\frac{C_{v_{1,1}}^{\text{mn.int}}}{C_{v_{1,2}}^{\text{mn.int}}} = 6.132$, 2) $\frac{C_{v_{2,1}}^{\text{mn.int}}}{C_{v_{2,2}}^{\text{mn.int}}} = 2.446$, 3) $\frac{C_{v_{1,1}}^{\text{mn.int}}}{C_{v_{2,1}}^{\text{mn.int}}} = 14.934$ and 4) $\frac{C_{v_{1,2}}^{\text{mn.int}}}{C_{v_{2,2}}^{\text{mn.int}}} = 5.956$. Here compassion the first and the second ratios implies the followings: in compare with the case $A < 0$ in case $A > 0$ the deceleration substantially lower that acceleration. At the same time compassion the third and the fourth ratios implies the followings: in compare with the case $A < 0$ in case $A > 0$ acceleration higher than deceleration. Therefore, all of these calculations imply that above noted circumstances will have major contributions in the formation of the sign of the leading coefficient *A*. On the base of these conditions it can be said that influence of the deceleration on the delay, environmental pollution and enhancement of the nose will be higher than in case of acceleration. Above we have developed traffic simulation and analysis the delays and the main parameters of kinematics, such as speeds, accelerations and deceleration of the vehicles moving through the additional entry lanes of the roundabouts. Regarding to this here we will do some comments concerning to this topic of our investigation. Analyzing the general Equation (2) represented acceleration and deceleration $a(s)$ shows that they have non-uniform rate of distribution over the full range of changing of *S*: $0 \le S \le S_{\min}$. Our literature search indicated significant influence, impact and effect of the delay and kinematics of vehicles' movement on such environmental factors as pollution and nose. Worsening of these two environmental factors substantively increasing especially in case of higher delays and harsh accelerations and decelerations. Regarding to modeling of pollutant concentrations and noises near roundabout area, incorporating the effects of acceleration and deceleration is an important consideration. It is desirable the determined pollution effect to be considered both velocity bounds and fluctuations, involved in acceleration and deceleration dynamics. Additionally, it has to be noted that the continuous growth of road traffic volumes, included roundabouts, leads to significant environment and economic problems. For this reason, there have been efforts for more than four decades to understand the dynamics of traffic flow in order to find ways to optimize traffic with respect to a reduction of environmental impacts and economical losses due to congestion. However, modern traffic control technology allows somewhat slow-down pollution due to delay, acceleration, deceleration and congestion. Our investigation identified that in case of negative leading coefficient *A*it takes place harsher deceleration (and related with it higher partial delay) than in case of positive *A*. It can be seen from our above calculations, where it shows that in case of $A<0$ the partial delay $t_{d(2,2)}$ and the estimated absolute values of decelerations $a(s)$ and $a(t)$ higher than in case $A>0$. Obviously, that in case $A<0$ it will take place higher environmental pollution and higher noise level expressed in decibels (dB).

Thus, applying the hypotactic-statistical model we simulated the movement of vehicles through the additional entry lane of roundabouts. This modeling allowed to find all of five constant coefficients of the sixth-degree polynomial function, represented the velocity of the vehicles moving through that lane. Then we thoroughly analyzed this function for its two different versions of presentation. In these two versions function's leading coefficient *A* had different values and different signs: one of them had positive sign and the other one negative. Based on these circumstances all kinds of delays, the kinematics and the dynamics of the moving vehicles have been investigated. It allowed to find velocities, accelerations, decelerations and delays for different intervals of movement of the vehicles. As it noted above based on these analyzes it was defined that in case of negative sign of the leading coefficient of the general Equation (1) the partial delay related to the decelerations $a(s)$ and $a(t)$ is higher and these decelerations are more harsher than in case of positive sign of the leading coefficient. In result of that here it takes place higher environmental pollution and increased level of noise.

4. Conclusion of the Calculations

Average delay reduction based on future configuration of the entire roundabout zones, mainly by means of adding of the circulating and additional entry lines. Quantifying and assessing the impact of flare or additional lane length on roundabout operation can be helpful to practitioners who are considering the use of adding a full lane in a roundabout design and to have a better understanding of the effectiveness of various lengths to roundabouts performance. Modeling the impact of additional lane length on roundabout operation and determination relationship between additional lane length and delay will be enabled to give recommendations on additional lane length design. Our calculations have been performed for the additional lane having enough long length (430 ft). However, as indicated in [1] shorter ($150\text{ ft} \le L \le 250\text{ ft}$) additional lane lengths are more effective in reducing delay than longer lengths (**Figure 5**). The national data on roundabout points out that roundabout delay can be decreased by either adding a full lane upstream of the roundabout or by widening the approach gradually (flaring) through the entry geometry (NCHRP 2010), but it does not give any guidelines on the length of the additional lane. This hypothesis aims to address the question of whether shorter additional lane lengths are more effective in reducing delay than longer lengths. Increasing the additional lane lengths allowed vehicles to use the extra space to reach the roundabout at a faster time thus increasing the speed. But when more vehicles enter the roundabout, the conflicting flow increases and, if there are still sufficient gaps in circulating traffic, more entering vehicles are able to enter at a faster rate, reducing delay. It is important to have enough capacity in the circulatory roadway to receive the entering traffic. The shorter lengths help regulate the rate of entry at a slow but constant rate than the longer lengths which can result in an instantaneous increase in circulatory roadway flow with less capacity to handle the flow. As shown in **Table 15**, a summary of research hypotheses (H_1, H_2 and H_3) results, regarding to designing of the additional lane of roundabout is presented.

Our calculations can confirm that additional lane length can be varied in a manner that effectively reduces delay without wasting money on unnecessary lane construction. This approach can also be used during the planning and design stage of a new roundabout in order to determine the appropriate additional lane length without expanding resources on the design and construction of unnecessarily long lengths. However, here additional analysis is needed to determine the effect of different lengths on safety since existing studies have shown that increasing the lengths increase speed on the approach to the roundabout. The main goal for modifying the old configuration of roundabouts was to reduce speed and thereby increase safety. If increasing the lengths results in increased speed, this could undermine the operational benefits of a modern roundabout. Therefore, determining an appropriate length allows the ability to identify an optimal additional length to improve operations with an implication of minimizing the increase in speed on the approach. Transportation professionals still

Table 15. A summary of research hypotheses results.

Hypothesis	Statement	Significant
H_1	Short additional lane lengths are more effective in reducing delay than longer lengths.	Yes
H_2	Adjusting the additional lane length has to be done concurrently with the exit lane length in order to reduce delay.	No
H_3	Adjusting the additional lane length on all legs is more effective in reducing delay than adjusting just one leg.	Yes

find the existing models to be inadequate in delay prediction during real world oversaturated conditions. Models that effectively model delay during oversaturated conditions need to be developed specifically for roundabouts. It must be very actual consideration of the delays (due to the additional entry lane of roundabouts) in context of the environmental pollution and enhanced noise level within round abounds area.

Acknowledgements

We are grateful to Professor Claudio Campana for his contribution in publishing of this paper. Professor Campana programmed and diagramed a figure regarding to the gain of delay. We are also grateful to former Adjunct Professor of Mathematics at University of Hartford Mr. Alex Ginzburg for programming and diagramming the other figures of this paper.

Conflicts of Interest

The authors declare no conflicts of interest regarding the publication of this paper.

References

[1] Hammond, S. (2014) The Effect of Additional Lane Length on Roundabout Delay. Open Access Dissertations, Paper 230. https://digitalcommons.uri.edu/oa_diss/230

[2] Hammond, S., Hunter, C. and Chang, K. (2014) The Effect of Additional Lane Length on Double-Lane Roundabout Operation. *Journal of Transportation of the Institute of Transportation Engineers*, **6**, 71-84.

[3] Hammond, S., Rat, A., Delle Monache, M.L. and Piccoli, B. (2018) Operational Performance of a Double-Lane Roundabout with Additional Lane Length Design: Lighthill-Whitham-Richards Model Analysis. *TRB* 2018—*Transportation Research Board* 97*th Annual Meeting*, Washington DC, 7-11 January 2018, 1-14.

[4] Muga, G., Sala Mayato, R. and Egusquiza, I. (2003) Time in Quantum Mechanics (Lecture Notes in Physics Monographs, Book 72). Springer Science & Business Media, Berlin. https://doi.org/10.1007/3-540-45846-8

[5] Bixel, A. and Apai, D. (2021) Bioverse: A Simulation Framework to Assess the Statistical Power of Future Biosignature Surveys. *The Astronomical Journal*, **161**, 228.

[6] Dumičić, K. and Žmuk, B. (2013) Use of Power Analysis in Choosing Appropriate Sample Size for Quality Inspection. *Poslovna Izvrsnost Zagreb*, **7**, 147-160.

[7] Maidala, A.Y, Odujoko, A.O., Sadjere, E.G. and Ariavie, G.O. (2017) Design of a Pipeline Leakage Detection System. *International Journal of Advanced Engineering Research and Science* (*IJAERS*), **4**, 103-110. https://doi.org/10.22161/ijaers.4.5.17

[8] Gotoda, H., Nikimoto, H., Miyano, T. and Tachibana, S. (2011) Dynamic Properties of Combustion Instability in a Lean Premixed Gas-Turbine Combustor. *Chaos*: *An Interdisciplinary Journal of Nonlinear Science*, **21**, Article ID: 013124. https://doi.org/10.1063/1.3563577

[9] Lehmann, E.L. and Romano, J.P. (2005) Testing Statistical Hypotheses. 3rd Edition, Springer, New York.

[10] Malik, M. (2006) Pitfalls of the Concept of Incremental Specificity Used in Comparisons of Dual Chamber VT/VF Detection Algorithms. *Pacing and Clinical Elec-*

trophysiology, **23**, 1166-1170. https://doi.org/10.1111/j.1540-8159.2000.tb00919.x

[11] Bunnefeld, N. and Phillimore, A.B. (2012) Island, Archipelago and Taxon Effects: Mixed Models as a Means of Dealing with the Imperfect Design of Nature's Experiments. *Ecography*, **35**, 15-22. https://doi.org/10.1111/j.1600-0587.2011.07078.x

[12] Li, Y., Wang, S.Y., Zhao, Q.H. and Wang, G.H. (2020) A New SAR Image Filter for Preserving Speckle Statistical Distribution. *Signal Processing*, **176**, Article ID: 107706. https://doi.org/10.1016/j.sigpro.2020.107706

[13] Abidin, N.Z., Adam, M.B. and Midi, H. (2014) Hypothesis Tests of Goodness-of-Fit for Fréchet Distribution. *Pertanika Journal of Science & Technology*, **22**, 419-432.

[14] Carfantan, H. and Idier, J. (2010) Statistical Linear Destriping of Satellite-Based Pushbroom-Type Images. *IEEE Transactions on Geoscience and Remote Sensing*, **48**, 1860-1871. https://doi.org/10.1109/TGRS.2009.2033587

[15] Dhivya, R. and Prakash, R. (2018) Stripe Noise Separation and Removal in Remote Sensing Images. *Journal of Computational and Theoretical Nanoscience*, **15**, 2724-2728. https://doi.org/10.1166/jctn.2018.7530

[16] Rahal, R. (2017) Time Series Modeling and Forecasting Using Genetic Algorithms. Thèse de Doctorat en Sciences, Djillali Liabes University, Sidi Bel Abbès.

[17] Clark, C.A. (1963) Hypothesis Testing in Relation to Statistical Methodology. *Review of Educational Research*, **33**, 455-473. https://doi.org/10.3102/00346543033005455

[18] Banks, H.T., Kapraun, D.F., Thompson, W.C., Peligero, C., Argilaguet, J. and Meyerhans, A. (2013) A Novel Statistical Analysis and Interpretation of Flow Cytometry Data. *Journal of Biological Dynamics*, **7**, 96-132. https://doi.org/10.1080/17513758.2013.812753

[19] Hu, X.M., Xu, Z.F., Cai, H.X. and Hu, J.J. (2014) Kinetic-Monte-Carlo-Based Parallel Evolution Simulation Algorithm of Dust Particles. *Journal of Applied Mathematics*, **2014**, Article ID: 839726. https://doi.org/10.1155/2014/839726

[20] Hu, X.M., Wang, B., Fan, B.B., Xu, Z.F. and Chang, J. (2014) Research on KMC-Based Evolution Simulation of Dust Particles in Virtual Campus Environment. *Simulation Modelling Practice and Theory*, **40**, 28-38. https://doi.org/10.1016/j.simpat.2013.08.006

[21] Hu, X.M., Li, M.H., Wang, C., Yang, X. and Wei, C.J. (2018) Visualization of Dust Evolution Simulation Model in Campus Environment. 2018 *IEEE* 3*rd International Conference on Image*, *Vision and Computing* (*ICIVC*), Chongqing, 27-29 June 2018, 941-946. https://doi.org/10.1109/ICIVC.2018.8492797

[22] Du, K., Wan, P., Wang, Y., Ai, X. and Chen, H. (2020) Spectrum Sensing Method Based on Information Geometry and Deep Neural Network. *Entropy*, **22**, Article No. 94. https://doi.org/10.3390/e22010094

[23] Alam, S. and McNabola, A. (2018) The Network-Wide Traffic and Environmental Impacts of Acceleration and Deceleration among Eco-Driving Vehicles in Different Road Configurations. *Transportation Planning and Technology*, **41**, 244-264. https://doi.org/10.1080/03081060.2018.1435436

[24] Kinzel, C.S. and Trueblood, M.T. (2004) The Effects of Operational Parameters in the Simulation of Roundabouts. *ITE* 2004 *Annual Meeting and Exhibit*, Lake Buena Vista, 1-4 August 2004, p. 15. https://trid.trb.org/view/742534

[25] Godavarthy, R.P., Mirzazadeh, B., Russell, E.R. and Landman, D. (2016) Roundabout's Impact on Nearby Businesses. *Journal of Transportation Technologies*, **6**, 181-191. https://doi.org/10.4236/jtts.2016.64018

[26] Analysis for Roundabout Entrance and Exit Geometry. 2012 ODOT Highway Design Manual, White Paper; Roundabout Entrance and Exit Geometry.

[27] Russell, E.R., Landman, E.D. and Godavarthy, R. (2012) A Study of the Impact of Roundabouts on Traffic Flows and Business. A Cooperative Transportation Research Program between Kansas Department of Transportation, Kansas State University Transportation Center, and the University of Kansas. Report No. K-TRAN: KSU-09-10.

[28] Xu, H.F., Zhang, K. and Zhang, D. (2016) Multi-Level Traffic Control at Large Four-Leg Roundabouts. *Journal of Advanced Transportation*, **50**, 988-1007. https://doi.org/10.1002/atr.1385

[29] Berg, C., Retting, R.A. and Myers, E. (2005) Continued Reliance on Traffic Signals: The Cost of Missed Opportunities to Improve Traffic Flow and Safety at Urban Intersections. Kittelson & Associates, Inc., Baltimore, MD.

[30] Peirisa, S., Corbenb, B., Nieuwesteegc, M., Gablerd, H.C., Morrise, A., Bowmanf, D., Lennéa, M.G. and Fitzharrisa, M. (2018) Evaluation of Alternative Intersection Treatments at Rural Cross-Roads Using Simulation Software. *Traffic Injury Prevention*, **19**, S1-S7.

[31] Al Momani, M. (2009) A Comparison of Traffic Flow Performance of Roundabouts and Signalized Intersections Using MITSIMLab. Master's Thesis, Near East University, Graduate School of Applied Sciences, Nicosia.

[32] Georgia Department of Transportation (2018) Georgia Dot Research Project 15-07. Final Report. Safety Evaluation of Roundabouts in Georgia.

[33] Mohapatra, D.R. (2015) An Economic Analysis of Improvement of Road Infrastructure: A Case Study. *European Academic Research*, **2**, 14636-14651.

[34] Mandavilli, S., Russell, E.R. and Rys, M. (2003) Environmental Impact of Kansas Roundabouts. *The Emerging Technologies in Traffic Operations Session of the* 2003 *Annual Conference of the Transportation Association of Canada*, St. John's, 21-24 September 2003, 25 p.

[35] Ahmed, H. and Easa, S. (2018) Optimization of Single-Lane Roundabout Geometric Design: Environmental Sustainability. *Proceedings of the CSCE* 2018 *Annual Conference*, *Fredericton*, Fredericton, 13-16 June 2018, 10 p.

[36] Inman, V.W., Shafer, T., Katz, B.J., *et al.* (2003) Field Observations of Path and Speed of Motorists at Double-Lane Roundabouts. 2*nd Urban Street Symposium*: *Uptown*, *Downtown*, *or Small Town*: *Designing Urban Streets that Work*, Anaheim, 28-30 July 2003, 16 p.

[37] Accelerating Roundabout Implementation in the United States—Volume III of VII: Assessment of the Environmental Characteristics of Roundabouts. Publication NO. FHWA-SA-15-071.

[38] Transportation Research Board (2010) NCHRP Report 672: Roundabouts: An Informational Guide. Second Edition. National Cooperative Highway Research Program.

[39] Fakhar, M. and Fattah, T.H. (2016) Calculation of Traffic Noise Emissions Based on a Digital Traffic Model. A Toolkit for Evaluation of Road Traffic Design with Regard to Traffic Noise Emissions. Master's Thesis, Chalmers University of Technology, Göteborg.

[40] Zhao, L.H., Malikopoulos, A.A. and Rios-Torres, J. (2018) Optimal Control of Connected and Automated Vehicles at Roundabouts. *IFAC-PapersOnLine*, **51**, 73-78. https://doi.org/10.1016/j.ifacol.2018.07.013

[41] Nazaryan, N. and Fang, F.C. (2020) Quantify the Relationship between Roundabout

Geometry and Delay. *International Journal of Traffic and Transportation Engineering*, **9**, 25-36.

[42] Teterina I.A. and Parsaev, E.V. (2019) The Method of Calculating Emissions of Pollutants from Road Transport in an Urban Environment. *MATEC Web of Conferences*, **298**, Article ID: 00084. https://doi.org/10.1051/matecconf/201929800084

[43] Yerramalla, A. (2007) Vehicular Emissions Models Using Mobile 6.2 and Field Data. Master's Thesis, Faculty of the Graduate School, University of Texas, Arlington.

[44] Estevez-Maurizi, L., Forsseni, J., Kropp, W. and Zachos, G. (2016) Isolating Key Features in Urban Traffic Dynamics and Noise Emission: A Study on a Signalized Intersection and a Roundabout. *INTER-NOISE and NOISE-CON Congress and Conference Proceedings*, Hamburg, 2862-3857.

[45] De Coensela, B., Cana, A., Degraeuweb, B., De Vliegerb, I. and Botteldoorena, D. (2012) Effects of Traffic Signal Coordination on Noise and Air Pollutant Emissions. *Environmental Modelling & Software*, **35**, 74-83. https://doi.org/10.1016/j.envsoft.2012.02.009

[46] Texas A&M Transportation Institute (2017) Air Quality Benefits of Nighttime Construction in Texas Non-Attainment Counties—Technical Report 0-6864-1.

[47] Adamidis, F.K., Mantouka, E.G. and Vlahogianni, E.I. (2020) Effects of Controlling Aggressive Driving Behavior on Network-Wide Traffic Flow and Emissions. *International Journal of Transportation Science and Technology*, **9**, 263-276. https://doi.org/10.1016/j.ijtst.2020.05.003

[48] Bokarea, P.S. and Maurya, A.K. (2017) Acceleration-Deceleration Behaviour of Various Vehicle Types. *Transportation Research Procedia*, **25**, 4733-4749. https://doi.org/10.1016/j.trpro.2017.05.486

[49] Teng, H., Yu, L. and Qi, Y. (2001) Analytical Tool for Measuring Emission Impact of Acceleration and Deceleration Lanes. Report No. FHWANJ-2001-024.

[50] Khondaker, B. and Kattan, L. (2015) Variable Speed Limit: A Microscopic Analysis in a Connected Vehicle Environment. *Transportation Research Part C: Emerging Technologies*, **58**, 146-159. https://doi.org/10.1016/j.trc.2015.07.014

[51] Xu, S., Guo, H., Zhang, H.H. and Liu, X. (2021) Research on Project Teaching Method of Vehicle Dynamics under the Background of New Engineering. *Open Access Library Journal*, **8**, e7157.

[52] Krauss, S. (1997). Microscopic Modeling of Traffic Flow: Investigation of Collision Free Vehicle Dynamics. Ph.D. Thesis, University of Cologne, Köln.